

Extreme Bad Weather, Large Atmospheric Electric Field Fluctuations and Anomalous Changes in the High Voltage Electric Power Network in Thrace, North-East Greece, during the Solar Activity and the Magnetic Superstorm of March 2012

[Goergios Anagnostopoulos](#)*, Anastasios Karkanis, Athanasios Kampatagis, [Panagiotis K. Marhavalas](#), [Sofia-Anna Menesidou](#), [Dimitrios Efthymiadis](#), Stefanos Keskinis, [Dimitar Ouzounov](#), Nick Hatzigeorgiu, Michael Danikas

Posted Date: 26 December 2023

doi: 10.20944/preprints202312.1937.v1

Keywords: Remote Sensing; Space Weather; Exterme Events; Solar-Terrestrial relationsnsp; Weather prediction; Atmospheric Electric Field; Geomagnetically induced lectric currents



Preprints.org is a free multidiscipline platform providing preprint service that is dedicated to making early versions of research outputs permanently available and citable. Preprints posted at Preprints.org appear in Web of Science, Crossref, Google Scholar, Scilit, Europe PMC.

Copyright: This is an open access article distributed under the Creative Commons Attribution License which permits unrestricted use, distribution, and reproduction in any medium, provided the original work is properly cited.

Article

Extreme Bad Weather, Large Atmospheric Electric Field Fluctuations and Anomalous Changes in the High Voltage Electric Power Network in Thrace, North-East Greece, during the Solar Activity and the Magnetic Superstorm of March 2012

Georgios Anagnostopoulos ^{1,*}, Anastasios Karkanis ¹, Athanasios Kambatagis ²,
Panagiotis Marhavalas ³, Sofia-Anna Menesidou ⁴, Dimitrios Efthymiadis ¹, Stefanos Keskinis ⁵,
Dimitar Ouzounov ⁶, Nick Hatzigeorgiu ⁷ and Michael Danikas ¹

¹ Department of Electrical and Computer Engineering, Democritus University of Thrace, Greece; ankark@ee.duth.gr, deythym@ee.duth.gr, mdanikas@ee.duth.gr,

² Thermal Power Plant of Operation Department, TPP Komotini, Greece, a.kambatagis@dei.gr

³ Department of Production and Management Engineering, Democritus University of Thrace, Greece; marhaval@pme.duth.gr

⁴ R&D Department, Ubitech Ltd., 11632 Athens, Greece; smenesid@ee.duth.gr,

⁵ Network Major Installations Department, Hellenic Electricity Distribution Network Operator, Athens, Greece, keskinis95@gmail.com

⁶ Institute for Earth, Computing, Human and Observing (Institute for ECHO), Chapman University, USA, ouzounov@chapman.edu

⁷ Space Sciences Lab, UC Berkeley, USA; nikos@berkeley.edu

* Correspondence: ganagno@ee.duth.gr; Tel.: +30-25410-20486

Abstract: In a recent paper, we extended previous studies on solar-terrestrial relationships by investigating the origin of the March 2012 heatwave in northeast USA. In the present study we check the possible relationship of solar activity with the early March 2012 bad weather in northeast Thrace, Greece. To this end, we examined data from various remote sensing instrumentation monitoring the Sun (SDO satellite), the Interplanetary Space (ACE satellite), the Earth's magnetosphere (Earth based measurements, NOAA-19 satellite), the top of the clouds (TERRA and AQUA satellites) and the near ground atmosphere. Our comparative data analysis suggests that: (i) the winter-like weather (rainfall, fast winds, decreased temperature) in Thrace started on 6 March 2012, on the same day as the heatwave starting in USA, (ii) during the March 2012 winter-like event in Thrace (6-15 March), the ACE satellite recorded enhanced fluxes of solar energetic particles (SEPs), while SOHO and PAMELA recorded solar protons at very high energies (> 500 MeV), (iii) Thrace experienced particularly intense cyclonic circulation, during periods of magnetic storms on 8 - 10 and 12-13 March, which occurred after the arrival at ACE of two interplanetary shock waves, on March 8 and March 11, respectively, (iv) at the beginning of the two above mentioned periods large atmospheric electric fields were recorded, with values ranging between ~2000V/m - ~1800V/m on 8 March, (v) the winter-like 8-10 March 2012 weather occurred after the detection of the main SEP event related with a coronal mass ejection released in the interplanetary space as a result of intense solar flare activity observed by SDO on 7 March 2012, (vi) the 8-10 March weather was related with a deep drop of ~63°C in the cloud top temperature measured by MODIS/TERRA, which favors strong precipitation. Finally, we analyzed data from the electric power network in Thrace (~41°N) and we found, for the first time sudden voltage changes of ~3.5kV in the electric grid in Greece, during the decay phase of the March 2012 superstorm. We discuss the winter-like March 2012 event in Thrace in terms of solar cosmic ray influence on the low troposphere mediated by positive NAO. Finally, we infer that the novel finding of the geomagnetic effects on the electric power grid in Thrace may open a new window into space weather applications research.

Keywords: extreme weather events; Solar-terrestrial relationships; geomagnetically induced currents; SEP; march 2012 events; NAO effects; Mediterranean cyclones; cloud top temperature

1. Introduction

1.1. Solar activity and the subsequent Space Weather as agents of variations in Earth's atmosphere

The solar influence on the Earth's climate has been studied for a long time. The historic Maunder minimum (MM), between AD 1650 and 1715 [1] and the Medieval warm period, around 1000 AD [2] are well known events at least in the space and the atmospheric physics communities. During the space era, Earth-based and satellite measurements have shown that interplanetary coronal mass injections (ICMEs) affect the whole atmosphere up to low altitudes (~2000 m above sea level)[3].

The Sun is the principal energy source of the atmosphere and biosphere. The Sun affects the earth's environment via electromagnetic radiation, solar energetic particle (SEP) events and solar wind plasma. The crucial question we address in relative science communities is whether solar activity may contribute to some extent in the enhanced number of dangerous extreme atmospheric events.

In a previous case study, we considered for the first time, the possible solar influence on extreme events, by comparing space weather and atmospheric parameters during the March 2012 heatwave (M2012HW) in northeast USA [4]. We found strong evidence that both the M2012HW and the historic March 1910 heatwaves were most probably caused by solar activity induced effects into the Earth's magnetosphere and atmosphere.

Global warming is considered to be the agent of the increased frequency in our times [5,6]. A CarbonBrief' report entitled "Attributing Extreme Weather to Climate Change" suggests that human activity has been raising the risk of some kind of extreme weather, in particular, the heatwave events [7]. Many authors interpret this statement in the sense that climate change should not be considered the sole cause of each one of the extreme weather events. According to these authors, some natural variations can also trigger extreme events [8 - 10]. Ref. [7] claim that no discernible influence owing to human activity has been found in ~10% of the extreme weather events and trends that they studied, while in a further 11% of the extreme weather events not a reliable conclusion could be reached.. Connolly et al., in a recent review paper entitled "How Much Has the Sun Influenced Northern Hemisphere Temperature Trends? An Ongoing Debate", claimed that the debate on "anthropogenic versus solar influence" has not yet reached a consensus, and further data analysis and theoretical discussion is needed [11].

In the present study we examine and compare data from a variety of remote sensing instrumentation monitoring the Sun, the Interplanetary Space, the Earth's magnetosphere, the top of the clouds and the near ground atmosphere in order to check the possible relationship of solar activity with the early March 2012 winter-like weather in northeast Thrace, Greece, as a continuation of a recent similar study concerning the origin of the March 2012 heatwave in northeast USA. Our data analysis provides a good evidence on the influence of the unusual March 2012 solar and interplanetary space conditions on extreme events in Thrace, Greece. Furthermore, we report, for the first time, sudden (within 1 second) voltage changes in the electric power network in Thrace / Greece, at middle latitudes (~41°N).

1.2. Coronal Mass Ejection activity

One of the most important solar phenomena is the coronal mass ejection (CME)[12]. Once a CME escapes from the Sun, it propagates in the interplanetary space and reaches the Earth's orbit at velocities ranging from ~350 km/sec up to ~2,000 km/sec. The time it takes a CME to arrive from the Sun to the Earth is about two days, although there are big variations as far as the duration time is concerned [13]. A CME expanding in the interplanetary space can create a shock wave (SW) accelerating particles to high (GeV) energies, which are observed as large particle fluxes around the SW, and are known as solar energetic particle (SEP) events. Whenever a CME erupts on the side of the Sun facing Earth, and the Earth's orbit intersects the path of the CME cloud, spectacular and sometimes hazardous effects are observed[5], [6]. An ICME reaching the Earth's magnetosphere induces geomagnetic disturbance, a magnetic storm, due to solar wind plasma pressure and southward interplanetary magnetic field (IMF) interactions with the magnetosphere / bow shock. The

arrivals of ICMEs on Earth can cause many physical processes to take place in Earth's magnetosphere [13 - 16], ionosphere [17, 18], atmosphere [4, 19, 20], lithosphere [21-23], biosphere [24 - 27] and technosphere [28 -30]. The most spectacular effect of ICMEs is the aurora, which appears as curtains, rays and spirals in dynamic variations in the sky, predominantly seen in high-latitude regions.

1.3. Solar Energetic Particles and tropospheric variations.

The research on solar–terrestrial relationships has emphasized solar cycle (≈ 11 -year periodicity) climate trends so far and has concentrated on stratospheric changes, polar variations, cloudy and sea / surface temperatures [19, 31]. Furthermore, it is accepted that solar activity affects both long-time (climate) and short- time (weather) variation [3, 11, 31 - 37].

Short-term meteorological responses to solar variable activity has been reported since the beginning of the space era [33]. For instance, Schuurmans [33] reported changes at the tropopause within 12 hours after strong solar flares and other tropospheric effects 2–4 days after the flares. Furthermore, Pudovkin and Raspopov [38] and Pudovkin and Babushkina [39], provided significant evidence that the main agent of weather variations in the lower atmosphere is the solar and galactic cosmic ray radiation.

Avakyan et al. [3] studied the meteorological variations at low height during the Halloween October 2003 solar events and they observed a T increase after large magnetic storms ($K_p > 5$) in 84% of the cases studied at an altitude of 2100 m (at the mountain meteorological observatory near Kislovodsk). Moreover, strong electric field fluctuations were reported after the 2013 Halloween events in Kamchatka, while many other researchers reported various other atmospheric reflections following the October 2003 solar events [40, 41]. In addition galactic cosmic rays appear to play a significant part in climate and weather [42 – 45].

In conclusion, various studies indicate that after a solar flare, tropospheric variations can occur in 2-4 days, i.e. the time required for a CME released into the interplanetary space to reach our planet.

1.4. CME related Geomagnetically Induced Electric fields and Currents on the Ground

During an ICME-induced magnetic storm the geomagnetic field changes. The induced electric field also creates currents in man-made conductor systems, such as telecommunication cables, electric power networks, oil and gas pipelines, and railway equipment; these currents have been called “geomagnetically induced currents” or GIC [28, 46]. GICs are related with surface voltages with values between ~ 1 V/km and ~ 5 V/km, with maximum values of ~ 20 V/km. [47].

The GICs are generally of the order of tens to hundreds of amperes. These quasi-DC currents are small compared to the normal AC current flowing in the network, but they can induce an enormous impact on the operation of transformers. GIC levels of only 1-10A can initiate magnetic core saturation in a transformer. The geomagnetic variations are slow (\sim mHz) compared to the frequency used in electric power transmission (50 or 60 Hz). Therefore when a GIC flows through a transformer, it acts as a DC current. Then, as a result, highly distorted transformer currents are injected into the electric power network [48].

Studies on the effects of solar eruptions on the Earth's electric field and, consequently, on electric power grids, began relatively recently, after a CME in 1979 [30]. The most famous GIC-induced electric failure occurred in the Hydro-Quebec power system in 1989 [47-50]. Although GICs usually appear at high latitudes, a large ICME may cause GICs at middle and even low latitudes. During the famous 2003 Halloween events, the magnetic variations produced an intense electric field on the ground across UK. After that event, the GICs raised significant concern within the power industry and government [51].

Liu et al. [14] attempted to identify the responses in low latitude China to space disturbances during a modest magnetic storm on 14 July 2012. They inferred that some transformers had more or less responses to the moderate storm depending on the type of the transformer and the grid, under similar geographical conditions (i.e. latitude, ground resistivity) [52].

As GICs increase, the level of saturation of an electric transformer core and its impact on the operation of the power network increases. For large storms, the spatial coverage of the magnetic

disturbance is large and a large number of transformers can be simultaneously saturated, a situation that can rapidly escalate into a network-wide voltage collapse. In addition, individual transformers may be damaged from overheating due to the unusual operational mode, which can result in long-term outages to key transformers in the network. Damage of these assets can slow the full restoration of power network operations [48]. Space scientists have strengthened their research in space weather prediction so that industry and states can avoid catastrophic effects in electric power systems.

In this study we will show, for the first time, that GIC disturbances in the electric network may affect the middle latitude southeast Europe as well. In particular we will present results from the electric grid in Thrace, northeast Greece, at $\sim 40^\circ\text{N}$, revealing voltage disturbances during the March 2012 space / atmospheric extreme events.

1.5. Vertical atmospheric electric field E_z near ground during magnetic storms

The atmospheric electric field (AEF) E_z is the field existing in the atmosphere due to the ground and ionosphere, which are negatively and positively charged, respectively. The AEF is formed by the potential difference of 250 kV between the ionosphere and the Earth's surface [53] and is directed vertically toward the ground, under fair weather conditions. Globally, the E_z value is approximately 100 V/m - 200 V/m [54, 55]. The variability in the atmospheric electric field is strongly dependent on a combination of conditions and it is divided into fair-weather AEF and disturbed-weather AEF.

The vertically orientated AEF E_z can be affected by weather conditions, soil morphology and solar activities [56]. The AEF can be also affected by thunderstorms [57, 58, 59], cloudiness [60], geomagnetic activities [61], solar activities [62, 63] and air pollution [64, 65]. Also, the environmental and meteorological differences in some places can affect the AEF [66 -70]. Furthermore, the AEF is influenced by earthquakes [71 -74].

Significant work has recently been based on the relation of disturbed AEF E_z with space weather. Among others, Kleimenova et al. presented the effect of 14 magnetic storm main phases in daytime midlatitude variations in the vertical component E_z of the atmospheric electric field, in the absence of local geomagnetic disturbances [75]. They reported, under conditions of fair weather, considerable (~ 100 – 300 V/m) decreases in E_z values at Swidermidlatitude Poland observatory (47.8°N), at times of substorm onset in nighttime auroral latitudes (College observatory). They inferred that an increase in precipitation of energetic electrons into the nighttime auroral ionosphere, can result in considerable disturbances in the midlatitude AEF.

Strong electric field fluctuations were reported, among others, by Smirnov et al. after the 2013 Halloween events in Kamchatka [40]. Michnowski et al. compared measurements made at ground level in both the Arctic (S. Siedlecki Polish Polar Station Hornsund, Spitsbergen, Svalbard, Norway) and at mid-latitudes (Swider, S. Kalinowski Geophysical Observatory, Poland) [76]. They inferred that the solar wind changes produce measurable effects on ground-level E_z and J_z at middle latitudes, dependent on the strength of the ICME-induced magnetic storms. These authors claimed that the almost-simultaneous detection of solar wind parameter changes, magnetic storms and variations in the E_z / J_z confirms their physical relationship.

2. Instruments and Data

The Solar Dynamics Observatory (SDO) was designed to understand the Sun's variability and its impacts on Earth. It was launched on February 11, 2010 (<https://sdo.gsfc.nasa.gov/>). The goal of this mission is to advance the predictive capability of solar influence on Earth's humanity and humanity's technological systems [77]. The SDO mission includes three scientific investigations: the Atmospheric Imaging Assembly (AIA), Extreme Ultraviolet Variability Experiment (EVE), and Helioseismic and Magnetic Imager (HMI). Here we use measurements from the Atmospheric Imaging Assembly (AIA) telescope taking images from the Sun every 10 seconds. In this study, images are examined in the passband of 4500\AA and 171\AA (<https://helioviewer.org>).

The space weather research is based on measurements obtained by the NASA Advanced Composition Explorer (ACE) satellite [78] (<http://www.srl.caltech.edu/ACE/>, accessed on 27 May 2022). ACE is circulating the L1 Lagrangian point (Figure 1), at a distance of ~ 220 RE from the Earth

(Figure 1; R_E is the length of the Earth's radius). (<https://www.swpc.noaa.gov/products/ace-real-time-solar-wind>, accessed on 27 May 2022). In the present paper we present energetic particle data from the EPAM experiment [4].

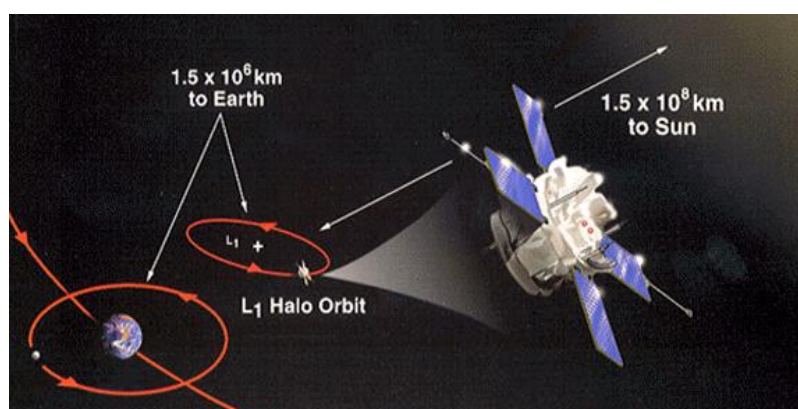


Figure 1. ACE circulating, around the L_1 Lagrangian point. The L_1 Earth-Sun gravitational equilibrium lies at a distance of $\sim 220 R_E$.

Terra is in a circular sun-synchronous polar orbit completing a revolution every 99 minutes. The Terra satellite explores the connections between Earth's atmosphere, land, snow and ice, ocean, and energy balance to understand Earth's climate and climate change and to map the impact of human activity and natural disasters on communities and ecosystems. It moves at an altitude of ~ 700 km with an inclination of 98.5° (<https://terra.nasa.gov>). Aqua is also in a circular sun-synchronous polar orbit with a period of 98.8 minutes, at an altitude of ~ 700 km with an inclination of 98.2° (<https://aqua.nasa.gov/content/about-aqua>) [79, 80]. The Moderate-resolution Imaging Spectroradiometer (MODIS) is a key instrument aboard the NASA's Terra and Aqua satellites to improve understanding of global atmospheric dynamics and processes occurring on Earth and its environment [81].

NOAA 19 is the fifth in a series of five POES satellites (Polar-orbiting Operational Environmental Satellites) circling at an altitude of ~ 850 km above Earth with a period of ~ 100 min.

The data used in our study for the determination of voltage variations in the high voltage 150kV transmission network are coming from the SCADA system of the Thermal Power Plant of Komotini, which is located in Thrace, Northern Greece [82].

3. Data analysis results

3.1. March 2012 extreme events

In a recent paper we have provided significant evidence that the March 2012 heat wave in northeast USA was affected by solar activity [4]. The conclusion was based on the comparison (i) of observations in the near Earth interplanetary space (ACE satellite at the Lagrangian L_1 point between Sun-Earth) and at the Earth's ground, (ii) of the March 2012 heatwave with the March 1910 heatwave, which occurred before the GHG effect and is understood as a non-anthropogenic, a natural event. The conclusion was supported by the elaboration of a CME – related heat wave in March 2015.

The March 2012 heat was not been a local, American extreme weather event. March 2012 is also known for extreme meteorological weather events occurring all over the globe. Here we examine the atmospheric weather in southeast Europe after the incident of a geoeffective coronal mass ejection, by incorporating remote sensing data revealing the spatio-temporal variations on the solar disk (SDO satellite) and on the top of the clouds (TERRA satellite). The space weather, which affects (and in some extent predict) the large scale electromagnetic environment of Earth (magnetosphere, ionosphere, atmosphere) is examined by using the ACE observations at the Lagrangian L_1 point between Sun-Earth, as in our study of the March 2012 heat wave [4]. In [4] we inferred that the

unusual space, magnetospheric, ionospheric and atmospheric events in March 2012 started after the appearance of the solar active region (AR) 11429 on March 5. Figure 2 shows images from the solar corona, obtained by AIA onboard SDO on March 7. Image 2a clearly shows the AR11429 at 00:00:08 UT in the passband of 4500Å (panel a) in the northeast site of the disk. The AIA telescope on the SDO satellite recorded a barrage of two X-class flares in rapid succession. The first flare was an X5.4 from N18° E 31°, starting at 00:02 UT on March 7th and peaking at 00:24 UT, while the second, at N15° E26°, was a X1.4 flare, which started at 01:05 UT and peaked at 01:14 UT. We note that an X2 flare is twice the strength of an X1 flare, an X3 flare is three times as powerful as an X1, etc., which suggests that X5.4 was an extremely intense solar flare.

The two images shown in Figure 2b,c were obtained by AIA in the passband of 171Å just before (00:04:24 UT) and after (00:24:48 UT) the X5.4 flare (peaking at 00:24 UT) and the comparison of the two images reasonably suggests the difference in brightness after 00:24 UT. Both flares, X5.4 (F1) and X1.4 (F2), were accompanied by two ultra-fast (>2000 km / sec) CMEs and highly disturbed the Earth's magnetosphere.

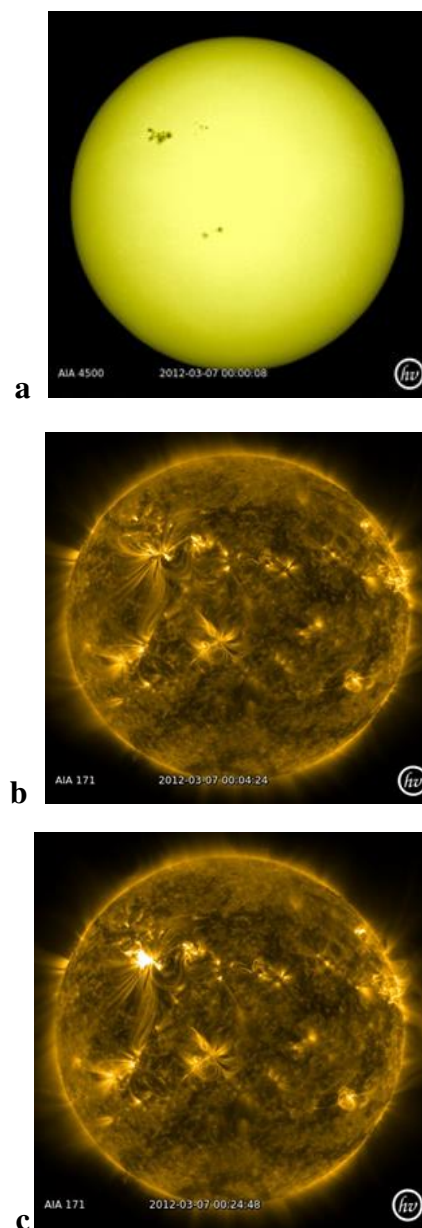


Figure 2. Images of the Sun obtained by the telescope Atmospheric Imaging Assembly (AIA) onboard the Solar Dynamics Observatory (SDO) satellite on 7 March 2012 in the passband of 4500Å (picture

a) and 171A⁰ (pictures b and c). Image a clearly shows the active region (at 00:00:08 UT), which was responsible for the intense ICMEs strongly affected the Earth's magnetosphere and atmosphere in March 2012. Images b and c were obtained just before (00:04:24 UT) and after (00:24:48 UT) the X5.4 flare (00:24 UT) on 7 March.

In Figure 3 we combine space and atmospheric weather data temporally related with the intense solar flares and the subsequent eruption of the two CMEs in March 2012; the two upper panels, a and b, provide information for the atmospheric weather in Alexandroupoli, Thrace, northeast Greece, and the two bottom panels, c and d, crucial information concerning the space weather near Earth (magnetosphere) and far upstream from the planetary magnetohydrodynamic (MHD) shock, which is the boundary between the magnetosphere and the interplanetary space (interplanetary space). In particular, Figure 3 displays time profiles of the daily maximum value of temperature T_A in Alexandroupoli (panel a), the rainfall in the same town (panel b), the fluxes of DE1 energetic (38–53 keV) electrons, and of both the P2' low (68–115 keV) and the P8 high (1880–4700 keV) energy protons as detected by the ACE satellite in the interplanetary (IP) space, around the Langragian point L1, (panel c; for the L1 point see Figure 1), along with the index Dst (panel d), from a network of near-equatorial geomagnetic observatories [83].

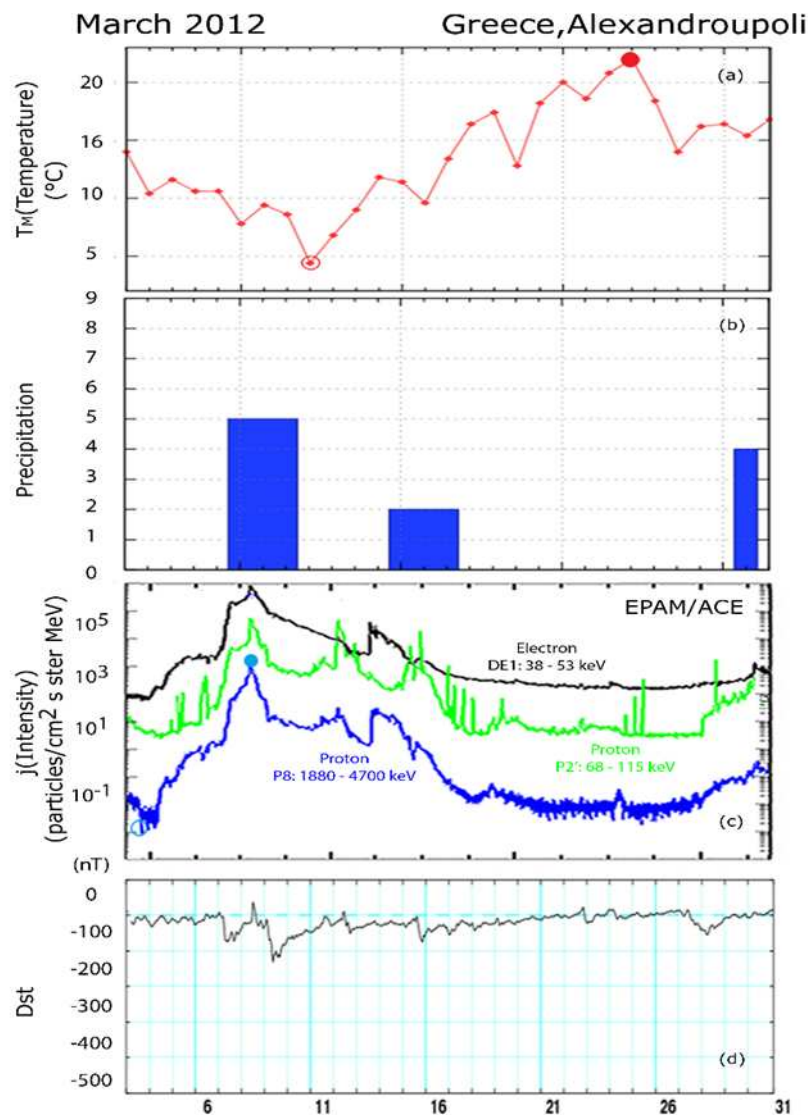


Figure 3. The data in the figure show three time intervals with rainfall in Alexandroupoli (blue bars in panel b) coincided with peaks in high energy solar proton P8 flux, around days 8, 14, and 30 of March 2012 (panel c)). During the period 6-16 March, when the energetic particles increased and then decreased, a superstorm occurred consisting of four individual storms on 7, 9, 11 and 15 March (panel d). At this period the temperature in Alexandroupoli decreased and then increased following in general the opposite pattern of the solar particles.

In panel d of Figure 3 we distinguish four magnetic storms, on days March 7, 9, 12 and 15, with low to very extreme low values of the geomagnetic index Dst. Tsurutani et al. [84] noted that storms S1, S2, S3 and S4 on March 7, 9, 12, and 15 appeared after ICME-associated MHD travelling interplanetary shocks on days 7, 8, 11–12 and 15 March.

The influence of space weather on Earth and its environment is most often considered in terms of geomagnetic activity (magnetic storms). However, solar or galactic cosmic rays are known to influence the atmospheric dynamics. In panel c we see some flux peaks superimposed on a large time-scale flux structure starting on March 4 and ending on March 20. We name the onset phase of the whole proton flux structure on days 4–6 as SEP-1. The solar energetic proton (SEP) events seen as particular flux enhancements on days 7–9, 11–12 and 13–15 March 2012, are called SEP2, SEP3, and SEP4, respectively. Both the magnetic storms S1, S2, S3 and S4 and the solar proton events SEP1-2, SEP3, and SEP4 are causally related with the appearance of AR11429 on the solar disk and the subsequent IP space disturbance, in particular, due to the CMEs accompanied solar flares F1 and F2.

The short-lived low-energy P2' proton peaks seen after 17 March are of magnetospheric origin; they are produced by particle acceleration within the magnetosphere and escape into the interplanetary. These low energy flux peaks show high peak-to-background flux ratio (j_p/j_b), with $j_p/j_b > 10^2$, which are unusual for upstream protons at the position of ACE [4, 85]. These high j_p/j_b values recorded far upstream from the Earth's bow shock strongly suggest that the magnetosphere was a very strong accelerator at those times.

The largest solar proton and electron flux enhancement in Figure 3, SEP-2, is characterized by a sharp peak on March 8 around the time of the ICME-related shock (panel c). In [4] we noted that the March 8 SEP event falls into a rare class of solar cosmic ray events. For instance, the P8 (1.88–4.70 MeV) protons show an unusual flux increase, with a maximum peak intensity $j > 10^4$ p (cm². sec. sr. MeV)⁻¹ and an extreme value $j_p/j_b > 10^6$ compared to the background P8 flux on March 4 ($j_p/j_b > 10^3$ compared to the pre-flare values of March 6.) Furthermore, we also mentioned that the SEP-2 P8 flux ratio j_p/j_b was rather the highest one among the CME-related SEP events observed during a period of 18 years (1997–2015) [4].

The solar energetic electrons, like the energetic ions, follow open IMF lines and precipitate in the high latitude magnetosphere, ionosphere and atmosphere, into the cusp, a region that is adjacent to the outer radiation belt (RB). The outer RB is a region rich in energetic electrons, which reaches higher densities during SEP events. Figure 4 shows the flux-time profiles of energetic electrons observed by the MEP90° detector of the NOAA-18 satellite during three periods, when NOAA-18 crossed the electron radiation belts and the cusp in the north magnetosphere throughout the whole SEP event lasting between 5–17 March 2012: on March 8 (panel a), 11 (panel b) and 13 (panel c). The two lines on the top of each panel indicate differential intensities ($\#el / (cm^2. sec. sr. keV)$) in the energy range 30–100 keV (multiplied by a factor of 10) and 100–300 keV. The line at the bottom of the panels a, b and c indicates the integral intensity ($\#el / (cm^2. sec. sr)$) of semi-relativistic (>300 keV) electrons.

The SEP-2 event was unusually strong. By comparing the flux-time profiles of energetic electrons in panels a, b and c we see a plateau on day 8 at high latitudes for as long as the IP shock-related energetic electron population was reaching the Earth's environment (Figure 3c), while the electron intensity shows an increasing drop in the middle of the whole structure in panels b and c whilst as the solar flux was decreasing between 8–17 March (Figure 3). Panel a manifests a rare event, with a cusp fulfilled with electrons in such a way (high electron intensities) that actually it cannot be separated from the outer radiation belts. The outer radiation belts can be well distinguished in Panels b and c as two distinct structures at the edges of the whole high latitude flux enhancements. The flux drop in the cusp between ~02:40–02:48 UT on March 2013 shows a >300keV electron flux difference of

more than 2 orders of magnitudes, between the outer radiation belts and the cusp, although the solar energetic electron background is quite high (Figure 3c).

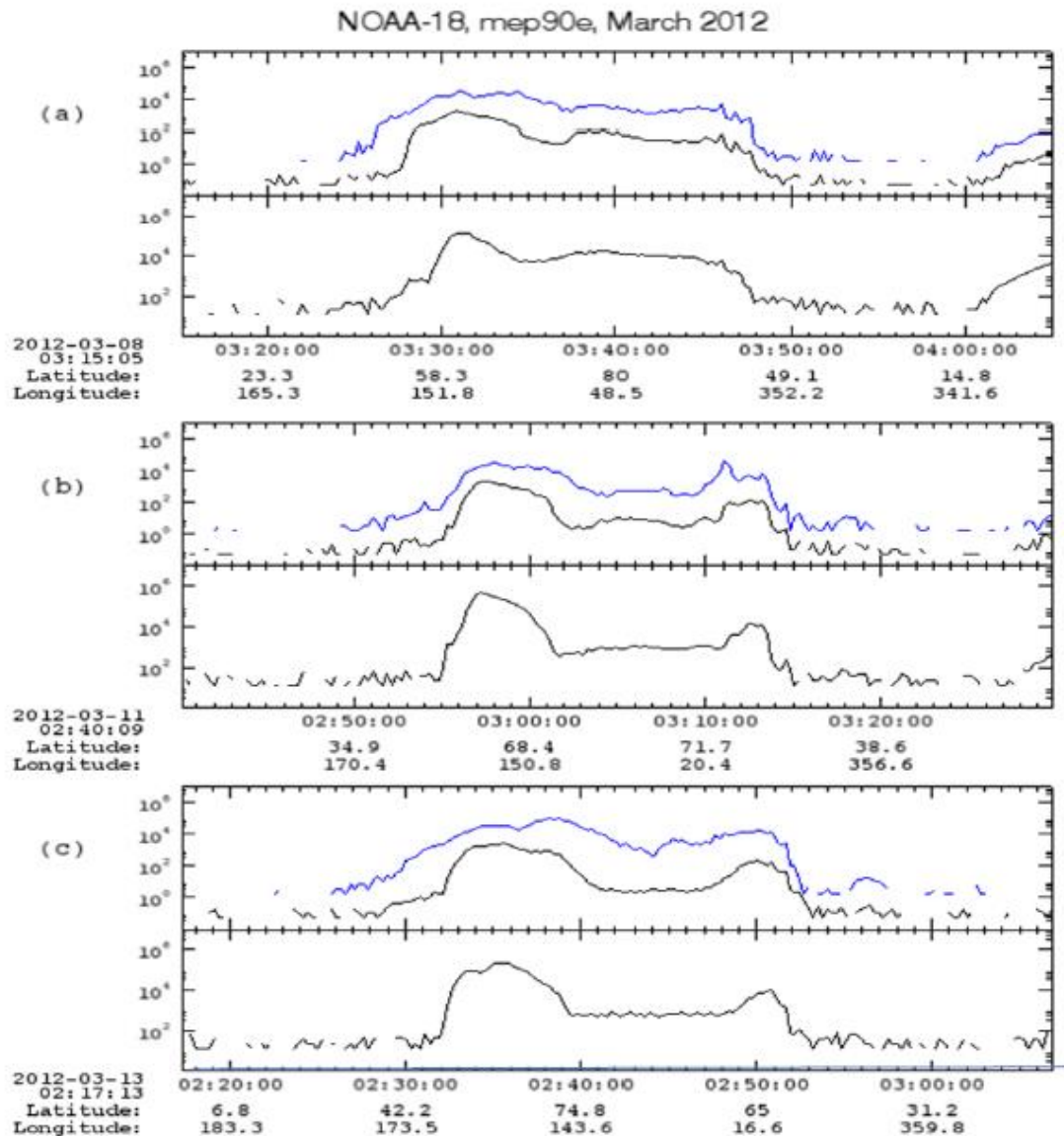


Figure 4. Flux-time profiles of energetic electrons observed by the MEP90⁰ detector of the NOAA-18 satellite during three periods on March 8 (panel a), 11 (panel b) and 13 (panel c). Panel a manifests a rare event, with a cusp fulfilled with energetic electrons in such a way (high electron intensities) that it cannot actually be separated from the outer radiation belts.

SEP events related with SF1 and SF2 were observed by a series of spacecraft located at various sites of the heliosphere and were observing protons to much higher energies than ACE. The SF1 / SF2 - related proton events observed within the magnetosphere by the GOES satellite showed a relative ~30 MeV proton flux enhancement >3.5 orders of magnitude (data not shown here). The solar cosmic rays observed by PAMELA during 7–9 March showed flux increases by a factor of $\sim 10^3$ at ~500 MeV [84], which suggests that the spectrum extends to energies much higher than 500 MeV. Protons with energies $E > 500$ MeV were also measured by the EPHIN instrument on the SOHO satellite [86]. The March 2012 solar activity was recorded at Earth as a very strong decrease in cosmic-ray fluxes on the ground after March 8 [87].

The impact of the March 2012 solar activity was so strong so that CMEs-related shock(s) drifted much of the solar system to heliocentric distances of ~124 AU [Gurnett et al. [88]. The March 7-related

CMEs were also detected at Mercury's orbit by Messenger, and they caused the most intense energetic particle flows during the cruise of the Mars Science Laboratory to Mars [89].

The energetic proton flux increase and a magnetic storm on March 28-30 seen in Figure 3c indicate remnants of particle reservoir still present in the next solar rotation originated from the SEP stream starting on 4 March.

3.2. *Extreme Meteorological Events in Thrace, northeast Greece, in March 2012.*

In [4] we provided significant evidence that the SF1 and SF2 and the subsequent release of highly geoeffective ICMEs were responsible for the March 2012 heat wave in northeast USA. It is well known that the March 2012 heat wave was not a local extreme weather event. Concurrent with the heat wave in northeast USA, western and central Europe experienced one of the warmest Marches. Temperatures in the U.K. recorded averages 4.5°F (2.5°C) above normal, i.e. the warmest March since 1957, while Austria and Germany had their third warmest March on record.

On the contrary, large parts of northwestern United States, western Canada, Alaska, eastern Asia, and Australia experienced below-average temperatures. March 2012 was also abnormally cool in southeast Europe. Heavy rains, snowfalls, and strong winds were observed during unusual winter-like spring weather in Greece. BBC NEWS website, for instance, describes the unusual March weather in Greece as follows: «Snowstorms have caused transport chaos around the Greek capital Athens, with one overnight traffic jam stretching for up to 15km (9 miles). Ferry services were disrupted and there were power cuts in some parts of the capital and on the islands, prompting some schools to close... Some roads in the Peloponnese, central Greece and the north of the country were also shut, according to the Greek news website Ekathimerini (<https://www.bbc.com/news/world-europe-12674491>)».

Since we found good observational evidence that the March 2012 heatwave in northeast USA was triggered by an unusual space weather following the SF1 and SF2[4], and we also know that weather anomalies were a global planetary phenomenon at that period [91], we wanted to check whether ground meteorological extremes in southeast Europe, Greece, were well related in time with specific space weather events, as in the case of the March 2012 [4]. This second case study was selected on the basis of the location of the University where most of the co-authors of this paper we work, the Demokritos University of Thrace (DUTH). DUTH extends over the geographical region of Thrace, in northeast Greece (Figure 4). Meteorological data in our study were obtained in two towns, in east and west Thrace, Alexandroupoli and Xanthi, respectively. A possible good relation of space weather with atmospheric extreme events at a specific second place on the globe (DUTH and its close region) in March 2012, besides the case of the March 2012 heat wave we previously examined [4], would greatly support space weather as the most likely candidate agent of the weather anomalies at the two sites on the globe (northeast USA - southeast Europe). Figure 5 displays a map of Greece. Alexandroupoli and Xanthi (marked by rectangles and indicated by solid red circles) are located at N40.846°, E25.874° and N41.13°, E24.89°, correspondingly in northeast Greece (southward of Bulgaria and west of Turkey).



Figure 5. Map of Greece. Ground measurements of weather parameters were measured in Xanthi, west Thrace, and Alexandroupoli, east Thrace. The two towns are marked on the map, in northeast Greece.

Firstly, we can see some characteristic features concerning a relationship between space weather at ACE, in the interplanetary space relatively near the Earth, and meteorological parameters in Alexandroupoli (east Thrace) in Figure 3. Rainfall in Alexandroupoli was recorded during three time intervals in March 2012: around days 8, 14, and 30 March 2012 (blue bars in panel b). A careful comparison of the data in Panels b and c suggests that rainfall in Alexandroupoli occurred during three major solar energetic particle (P8) flux enhancement that is around day 8-9 (SEP-2), 15-16 (SEP-4) and 30 March. Secondly, from the comparison of the data in Figure 3 we infer that during the period 6-16 March, when the energetic particle flux increased and then decreased, a superstorm was occurring (panel d), after the incident of CME-related MHD shock waves / SEP events starting on 7 March. Furthermore, at this period (6-16 March) the temperature T_A in Alexandroupoli decreased and then increased following in general the opposite pattern of the solar particles. In particular the temperature decreased until March 11 and fall from 15° to 3°C , that is a T_A variation $\Delta T_A = -12^{\circ}$, between 3-11 March. Then the temperature increased from 3° to 23° , that is an increase $\Delta T_A = 20^{\circ}$, until the end of the SEP event and beyond. We infer that the meteorological and space weather data in Figure 3 are consistent with space weather as an agent of the winter-like weather in Alexandroupoli between 6-16 March. This conclusion is further checked with more data from space and Earth based measurements in the following.

In Figure 6, we present Cloud top temperature (CTT) as made by the MODIS (Moderate Resolution Imaging Spectroradiometer) instrument onboard the Terra (Figure 6a and Aqua satellites (Figure 6b). The CTT 1-day mean measurements of Figure 6a and 6b were obtained by the Terra and Aqua satellites in the region enclosed in rectangle of Figure 5c (18.3181E, 33.2746N, 26.5359E, 42.1076N). The CTT values are shown in colors corresponding to those of the color bar on right side of Figure 6b, in a range from 1 to 30 March 2012 (horizontal axis).

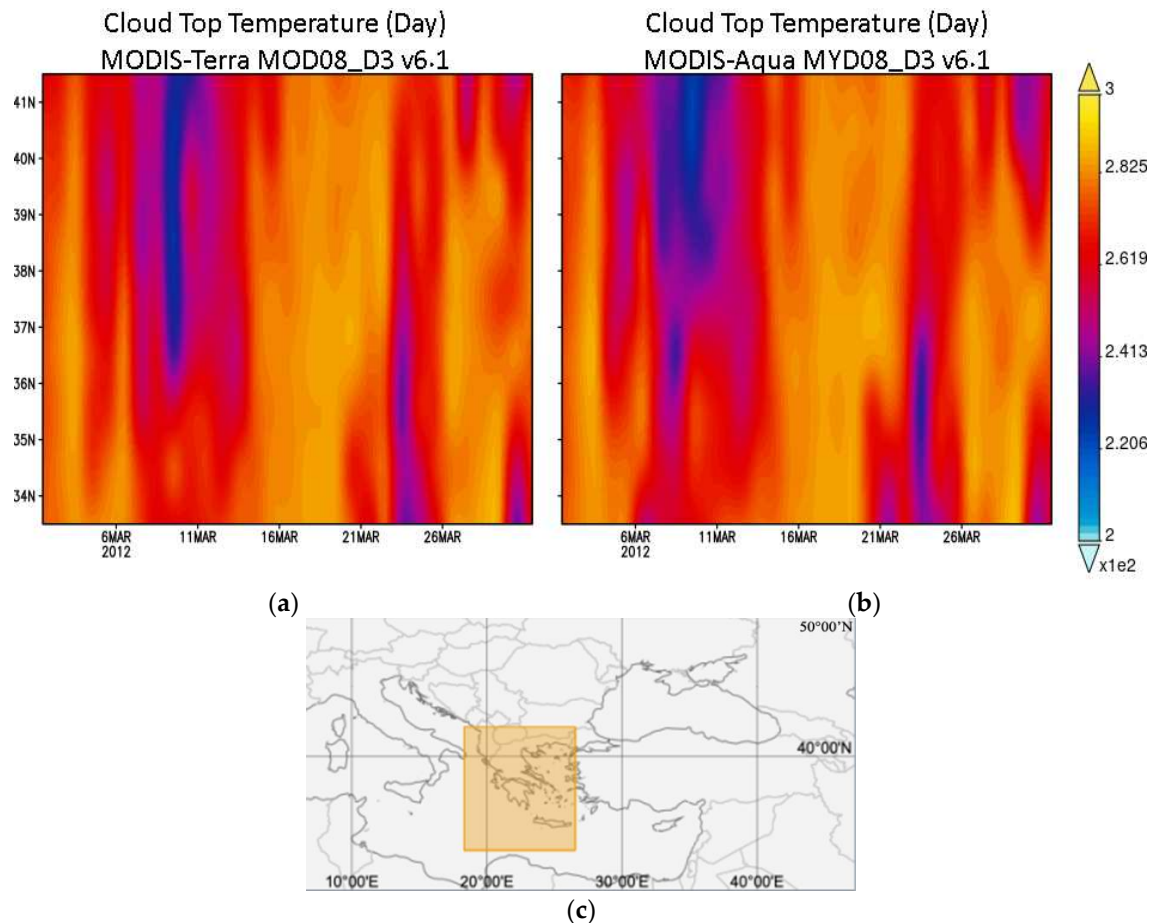


Figure 6. Cloud top temperature (CTT) as measured by MODIS (or Moderate Resolution Imaging Spectroradiometer) aboard the TERRA and AQUA satellites during the period 1 - 31 March 2012 in a region with latitudes between N33.5° – N41.5°. The lowest values were recorded by AQUA above north Greece between ~8-11 March during the major SEP-2 event of Figure 3c. The CTT color bar is in K (Kelvin). Analyses and visualizations using the MODIS Cloud top temperature (CTT) were produced with the Giovanni online data system, developed, and maintained by the NASA GES DISC.

From Figures 6a and 6b, the Hovmöller-Longitudinal Average projections represent essential spatial and temporal CTT features. Alexandroupoli is located at 40.85°N. The most striking feature is the bluish-colored structure at north latitudes centered at ~40° and extending ~50 southward. A careful look at the colors of the blue- structure suggests that TERRA/ MODIS and AQUA/MODIS reached very low values between on 9-11. 2012 and ~8-11.3. 2012, correspondingly. A comparison of the CTT values of Figures 5a,b with Figure 3c suggests that the lowest cloud-top temperature above Greece was recorded after SEP-2, which occurred on 7 - 8.3.2012, when the highest flux of protons in March 2012 was observed by ACE. Figure 5a shows a stable anomaly in decreasing the CTT around 9-11 March with a distinct level in comparison to the average level of CTT for the entire month of March 2012. The PM map for MODIS CTT (Figure 6b) shows a diffusion in the CTT level over the same spatial segment. This could be an effect of the afternoon migration of some humidity via the jet stream flow from the sea towards the land and facing the cloud formation but maintaining anomalies' patterns. After some additional checks with data a year before (March 2011), MODIS CTT maps for the same region show no similarities to the 2012 MODIS CTT (Appendix C). This suggests that the 2012 drop in CTT during March 9-11 is not affected by climatology or some usual seasonal pattern in the region.

In Figure 7 we examine the progress of the wind situation for fifteen days (March 3, 2012 - March 17, 2012). In particular, Figure 7 displays daily wind fields in south Europe and the Mediterranean Sea, including Xanthi, Greece (solid red circle), as described by NCEP Reanalysis at mid-tropospheric heights (500 hPa).

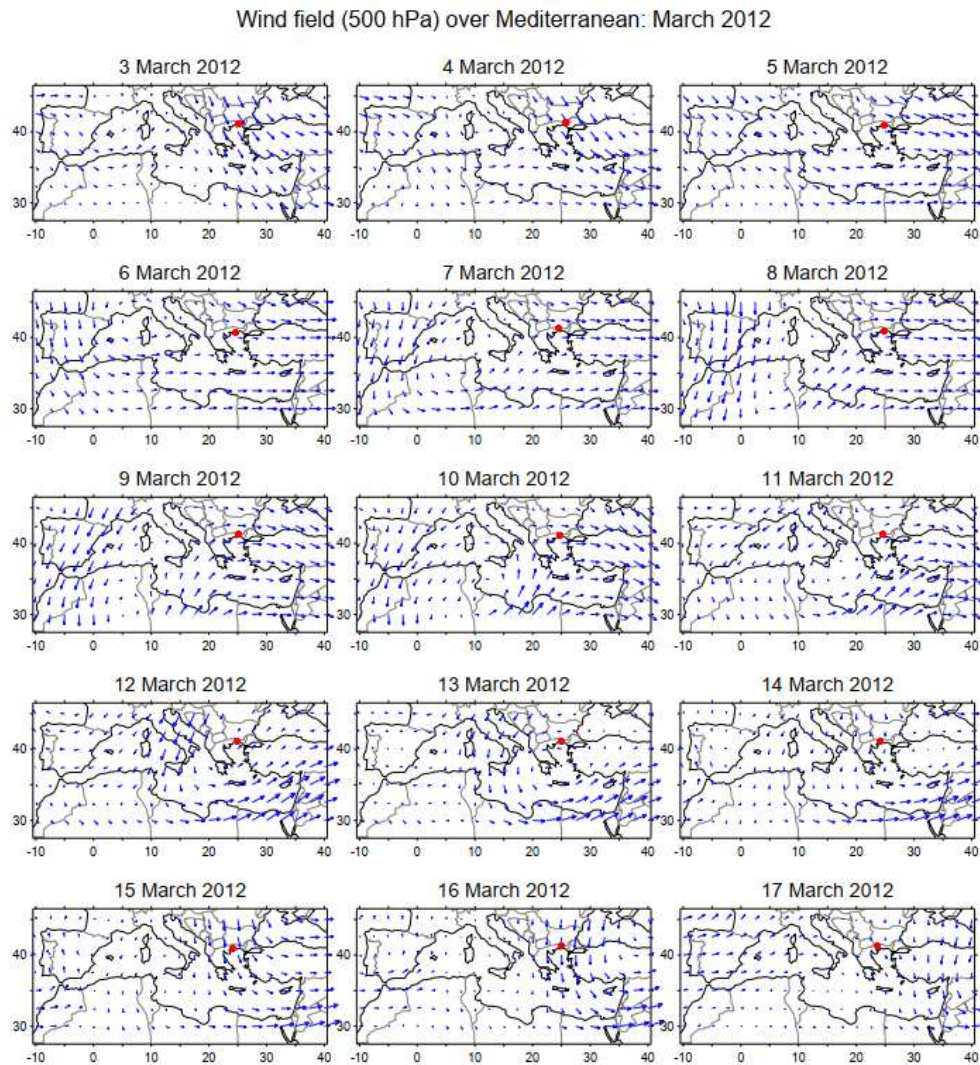


Figure 7. NCEP Reanalysis-provided daily wind fields at mid-tropospheric heights (500 hPa) for 3–17 March 2012. The location of Xanthi, Greece, is shown by a solid red circle. Thrace (solid red circle) experienced particularly intense cyclonic circulation, during periods of ICME-related magnetic storms on 8 - 10 (northward streaming) and 12-13 March (southward streaming).

Figure 6 shows that the speed wind intensifies during two phases (8 – 10.3.2012 and 12 – 13.3.2012) throughout the continuous course of an eastward moving cyclone appearing on March 6th in east Atlantic / west Mediterranean Sea and leaving the east Mediterranean / Middle East on March 17th; the two phases of the intensified wind speed coincide in time with the periods following the interplanetary shocks of 8 and 11 March probably suggesting a causal effect.

The wind fields indicate that strong southwesterly winds prevailed in the central Mediterranean on days 8-10, favoring the transfer of moist air from the central Mediterranean into the Greek territory. These winds were further reinforced by a cyclone which initially developed southwest of Greece and then moved northwards into the Greek area. The combination of the moist air and the subsequent low pressure conditions over Greece (allowing the uplift of the moist air) set favorable conditions for rainfalls in the Greek territory. These conditions coincide in time with the very low cloud top temperatures recorded by MODIS on TERRA and AQUA on March 8-11 at a long range of latitudes (Figures 5 and 6), after the arrival of the major SEP-2 event (March 7-9.3.2012).

In Figure 8 we present CTT measurements made by the MODIS instrument onboard the TERRA satellite, but at the Xanthi longitude. CTT are indicated as a function of latitude and time, in the range from N30° to N70° (horizontal axis) and from 4 to 13 March, 2012 (perpendicular axis), respectively. The T values are shown in colors corresponding to those of the color bar seen below the figure.

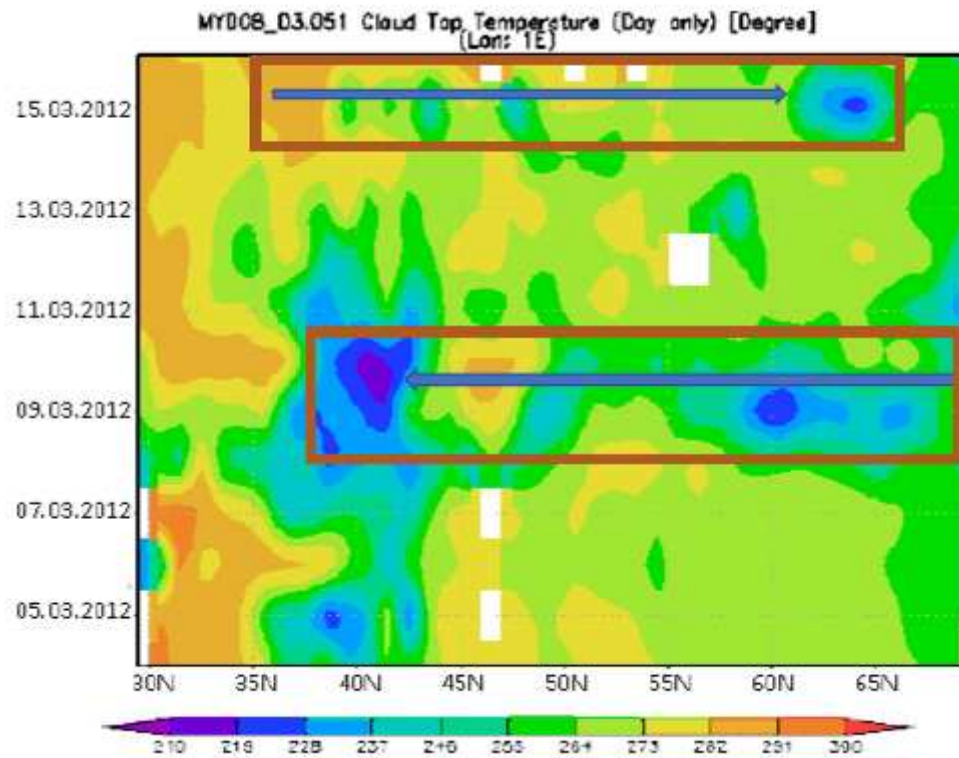


Figure 8. Top cloud temperature T as measured by MODIS (Moderate Resolution Imaging Spectroradiometer) aboard the Terra satellite, during the period 5 - 15 March 2012 in a region with latitudes between $N30^{\circ}$ – $N70^{\circ}$. The lowest T values were recorded above north Greece, at middle latitudes ($\sim 41^{\circ}N$), between ~ 9 -11 March during the major SEP-2 event of Figure 3. It is worth noting that the CTT drop structure recorded by MODIS / TERRA on 8-11.3.2012 (T1) appears to be a large structure over the middle and high latitude Europe, at Greece longitudes ($\sim 40^{\circ}$), extending all the way from $\sim 35^{\circ}N$ to $>70^{\circ}N$, which is consistent with the large scale extreme events appearing in the globe (i.e. heatwave in northeast USA [4]).

From Figure 8, we can see some important spatial and temporal features. The most striking feature is the blue colored structures on days 8-10.2012. A comparison of the T values of Figure 6 with SEP fluxes in Figure 3c suggests that the lowest cloud-top temperature above Alexandroupoli started recording by MODIS / TERRA after ~ 1 day from the onset of the SEP-2 event, that is about 1 day after the arrival of the March major SEP-2 event that was observed by ACE (7 - 8.3.2012), although low CTT are seen on day 7 as well.

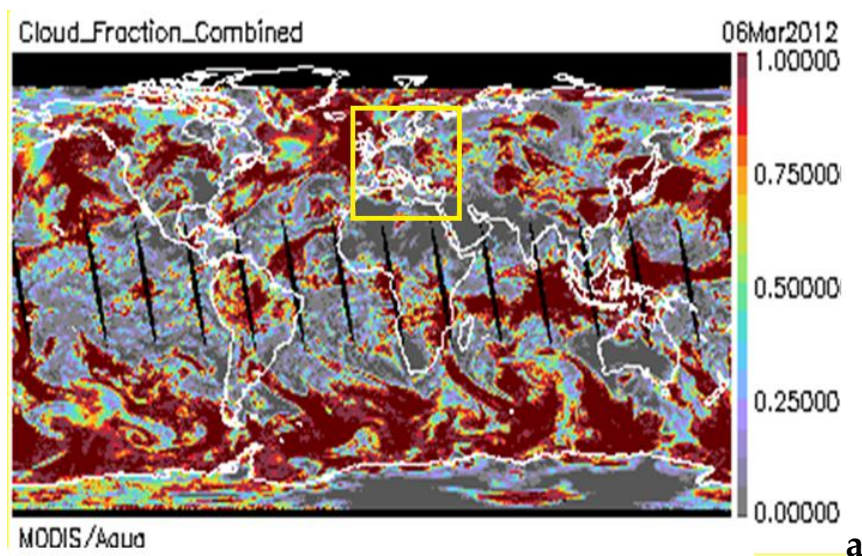
Furthermore, it is worth noting that the TTC drop structure was recorded by MODIS at a region of longitudes centered at $\sim 40^{\circ}$ and extending $\sim 5^{\circ}$ northward and $\sim 5^{\circ}$ southward. A careful look at the colors of the blue-green structure seen between 4 – 15 March 2012 suggests that the temperature T ranged between $\sim 0^{\circ}C$ - $\sim 63^{\circ}C$ ($\sim 210^{\circ}K$ – $\sim 273^{\circ}K$). Therefore, we infer that between 4 – 13 March 2012 the top of cloud above Alexandroupoli, was much cold suggesting appropriate conditions for precipitation [92].

A second T drop (green colors) in Figure 8, around Alexandroupoli's latitudes was recorded between the middle of days 14 and 15 March. This temperature decrease on the top of the clouds was recorded again ~ 1 day after the arrival of the SEP-4 event (~ 13 -15.3.2012), the second major particle event seen in Figure 3c.

It is worth noting that the CTT drop structure recorded by MODIS / TERRA on 8-11.3.2012 (T1) appears to be a large structure over the middle and high latitude Europe, at Greece longitudes ($\sim 40^{\circ}$), extending all the way from $\sim 35^{\circ}N$ to $>70^{\circ}N$, which is consistent with the large scale extreme events appearing in USA and the north Atlantic [4] and the global character of meteorological extreme

events at those times [91]. It is also worth noting that the second period with CCT drop, between 13-15.3.2012 (T2) suggests a large region with CCT decrease, but this event, T2, is slighter than T1, and shows minimum CCT at high latitudes around 65°N. In Figure 6 we show (by blue arrows in red rectangles) the general opposite CCT gradient direction between T1 and T2 events.

Figure 9 displays the cloud cover all over the planet according to the MODIS/Aqua measurements on 6 March 2012 (panel a) and 10 March 2012. Panels a and b indicate the cloudy covering of Earth before (March 6) and after (March 10) the arrival of the arrival of the ICME-related SEP-2 event, which bombarded the Earth's environment, in particular the cusp, with a flood of high energy ions and electrons (Figures 3 and 4). We have already discussed in [4] the large scale atmospheric dynamics in northeast America and the north Atlantic, characterized by an anti-cyclone in the north Atlantic providing warm air transported from the Gulf of Mexico in the northward direction. Figure 6 helps us to realize the large scale weather variation taking place from 6 to 10 March 2012 eastward from the north Atlantic anti-cyclone, in the whole region from northern Africa to the northern Europe (yellow rectangle). We see that the clear sky over almost the whole of Europe on March 6 (panel a) changed dramatically into a much cloudier sky above northern Africa, the central Mediterranean, the southeast Europe and a broad region inside the north European coasts after the ICME-related SEP-2 event (Figure 3), on March 10 (panel b; brown colored areas). Furthermore it is worth noting that in some European countries, like Belarus and Norway the rainfall started on March 10, while some areas experienced precipitation earlier, as for instance Hamburg, Germany (on March 7).



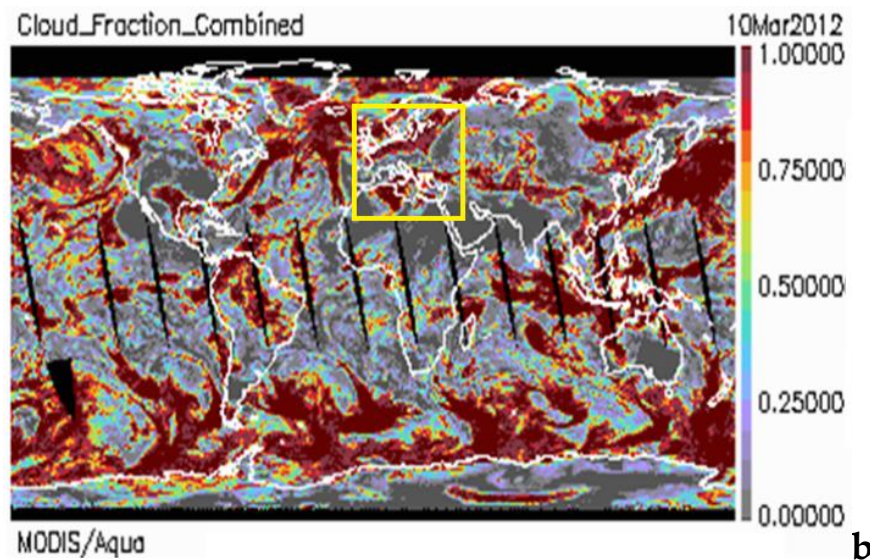


Figure 9. Cloudy all over the Earth according to the MODIS/Aqua measurements on March 6, 2012 (panel a) and March 10, 2012 (panel b). The clear sky over almost the whole of Europe on March 6 (panel a) changed dramatically into a much cloudier sky above the north Africa, the central Mediterranean, the southeast Europe and a broad region inside the north European coasts on March 10 (panel b; brown colored areas), after the detection of the ICME-related SEP-2 event by ACE (Figure 3).

The cloud cover shown in Figure 9 is consistent with the cloud top temperature seen in Figure 8 and suggests the existence of a large scale atmospheric anomaly that affected northern Africa, the Mediterranean and the Aegean Sea, the southeastern and northern Europe and the north Europe on March 10. Furthermore, the cloudy in the Mediterranean, the Aegean Sea, northern Africa and the southeastern Europe –including Greece– is consistent with the enhanced wind speeds of the anticyclone extending over these regions, as we saw in Figure 7. We recall that these weather disturbances occurred after the detection of the shock-related SEP event by ACE on March 7-8 and during the consequent large magnetic storm onset on March 9.

Figure 10 displays detailed meteorological measurements (courtesy of Pr. Kourtidis and Dr. Kastelis) from a station on the Campus of our Democritus University of Thrace (41.15° N, 24.92°E, 75m above sea level), in the town of Xanthi, ~90 km westward of Alexandroupoli (40.8° N, 25.8°E, Greece). The station is located approximately 3 km from the city center of Xanthi; thus, it is characterized as rural, and the city does not influence it. In particular, the measurements in Figure 8 show in detail the values of the atmospheric Potential Gradient (PG; [93, 94] of the electric field (red line), the wind speed (black line), and the accumulated precipitation (purple shaded region) during the period 5 – 15 March 2012. Figure 8 displays values of the electric field, of the wind speed and of the accumulated precipitation, which obviously suggests extreme bad weather starting on March 8 and continuing until the end of the time interval examined (March 15, 2012).

From Figure 10 we see that the meteorological station in Democritus University of Thrace recorded three large amplitude electric field fluctuations after the two IP shocks detected by ACE at ~1130 UT, on March 8 and at ~1228 UT on March 11, and the maximum SYM-H at 07:58 UT on March 9 as reported by [84]. Important to note is that the unusual large amplitude electric field fluctuations in the second half of March 8, ranging between ~-2000V/m - ~1800V/m, appears after the strong March 8 IP shock. It is also worth noting that both shock-related EFFs (~1130 UT on March 8 and ~1228 UT on March 11) show a fluctuation profile reaching large positive and negative values. On the contrary, the S2 magnetic storm-related AEF displays only negative electric field excursions at low values (of ~ 1000 V/m).

The IP shock-related AEFs on 8 and 11 March show unusually large amplitudes; they were stronger than the values of the EFFs recorded after the great Halloween events, which were recorded in Kamchatka on 28 and 30 October 2013 [95]. Such differences may be associated with either the peculiarities of local physical processes in the near-ground atmosphere or differences of registration locations [40].

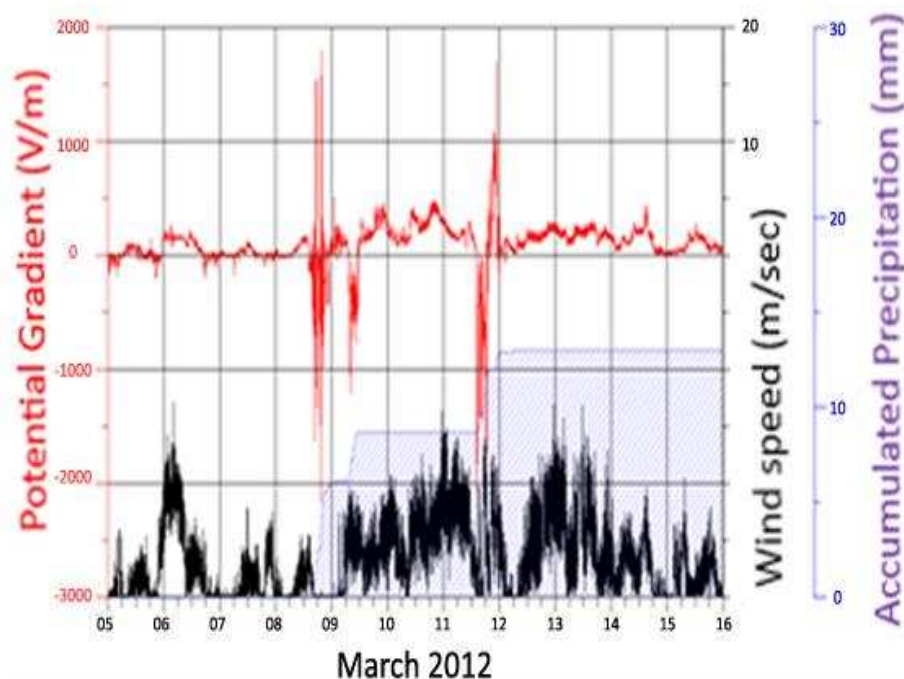


Figure 10. Atmospheric Potential Gradient (PG) of the electric field (red line), the wind speed (black line) and the accumulated precipitation (purple shaded region) between 5-15 March 2012. In the second half of days March 8 and 11 large fluctuations of the atmospheric electric field were recorded after the incident of two interplanetary shocks on the Earth. The AEF fluctuations were accompanied by winds and rainfall.

Figure 8 clearly shows that the 8, 9 and 11 March EFFs were followed by rainfall and winds (purple and black lines). It is worth noting that the increases in the accumulated precipitation were larger after the shock-associated bipolar EFFs than after the storm-associated negative electric field anomaly.

The space and terrestrial data shown above suggest that the extreme meteorological events occurring in March 2012 and in particular between 8-11 March were related with unusually intense solar activity and special weather events, as in the case of the March 2012 heatwave in northeast USA.

3.3. Perturbations in the High Voltage electric power grid in Thrace, Greece, in March 2012.

Since we have found good evidence of correlations between unusual meteorological variations in Thrace (Xanthi, Alexandroupoli), Greece, and the ICME-related SEP events in March 2012 that followed the occurrence of SF1 and SF2, in this section we examine the possible influence of space weather on the electric grid in the same region and at the same time period.

For this reason we investigate the possible relations of the March 2012 space weather events with possible perturbation in the high (150 kV) voltage electric power network in Thrace, north-east Greece, as recorded by the SCADA system of the Independent Power Transmission Operator (IPTO), in Komotini. Komotini is a town located between Xanthi and Alexandroupoli and is the capital of the local geographical region of Thrace. This second study of the present paper concerns the time period of March 5-15, 2012, which includes the major space weather events observed after SF1 and SF2 (Figures 2 and 3).

Since a series of papers have shown that during the incident of intense ICMEs on Earth's magnetosphere are often recorded as geomagnetically induced currents (GICs), which cause inconveniences to the electric power systems, we wanted to examine whether the electric IPTO grid in Thrace was affected by the geoeffective superstorm of March 2012, and, furthermore, if the agent of the possible electric current perturbations might be separated from the unusual meteorological events taking place in the same time period.

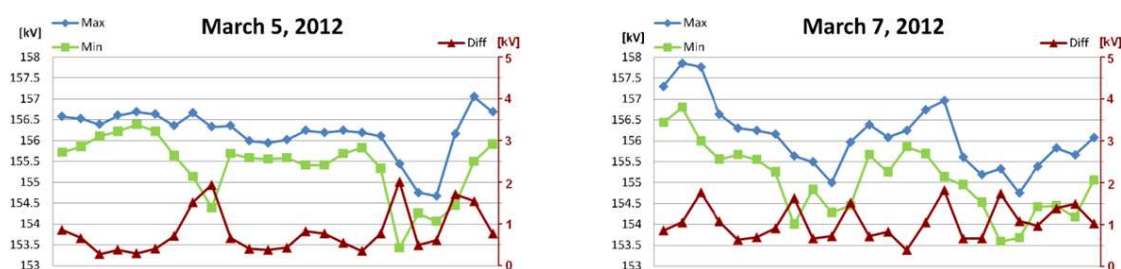
The IPTO factory's SCADA system records the voltages between the phases L1-L2, L2-L3 and L3-L1 in the connection point of the voltage output from the factory with the high voltage electric power grid every 1s. In the present study we analyze 1s and 1-hour of such averaged data. So, in Figure 11 we show 1-hour averaged data for selected days during the time period March 5-15, 2012. The data shown were created by processing the time-average values of the three 1s voltages between the phases L1-L2, L2-L3, L3-L1. From the 3600 values per hour, the maximum MAX (blue lines) and the minimum MIN (green lines) values per hour were determined. Furthermore, from the MIN and MAX values we also created time series of the differences (DFR = MAX – MIN) between the 1-hour averaged maximum and minimum voltage values. In Figure 9, the presented DFR values show the result of the actual DFR values added to the level of the 153kV standard voltage value (red lines) to avoid confusion with the other (MAX, MIN) lines.

Panels a and b on the left sides of Figure 11 present the 1-hour MAX, MIN and DFR voltage values on days 5 and 14 March, which were recorded under quiet magnetic conditions (Figure 3), well before and after the major SEP-2 event observed on days 7-9.3.2012 (Figure 3c).

The elaboration of the graphs in panels a and b reveals the appearance of a daily cycle of voltage changes in the 150kV transmission network at periods around 7:00LT - 9:00LT and 18:00 LT - 20:00 LT. The MIN voltages in the early morning hours (7:00LT - 9:00LT) correspond to times when inhabitants of Northern Greece are preparing to go to their place of work, while the MIN values in the afternoon hours (18:00 LT and 20:00 LT) correspond to times when the workers return homes, coinciding with the night darkness start; in the morning hours (7:00 LT - 9:00 LT), the night-lights turn off and the companies' activity start, and in the evening hours (18:00 - 20:00), the night-lights turn on due to household and public lighting activation. The peaks in DFR voltage (red line) at the 150kV transmission network in the morning and the afternoon, were unveiled on both days 5 and 14 March and they were present in all daily graphs checked for the interval 4-15.3.2012 (data not shown here).

Panels c and d, on the right side of Figure 11, show the 1-hour averaged MAX, MIN and DFR voltage values obtained by IPTO during days 7.3.2012 and 10.3.2012 and they are presented in the same format as in panels a and b. During these two days, 7.3.2012 and 10.3.2012, the Dst index reached low values (Figure 3d) suggesting that magnetic storms were in progress, due to the arrival of SEP-2 and the associated ICME, respectively. It is obvious that the MAX, MIN and DFR voltage profiles during the two storms (panels c and d) are different from those during the magnetically quiet days (panels a and b).

In particular, we see that the two large DFR peaks in the morning and in the afternoon of the quiet days divided into several voltage peaks of comparable values during the magnetically disturbed days 7.3.2012 and 10.3.2012. It is also remarkable that the general DFR background increases in prenoon-noon-afternoon times (11UT- 18UT) on March 10th, that is during the recovery phase of the major magnetic storm of March 2012.



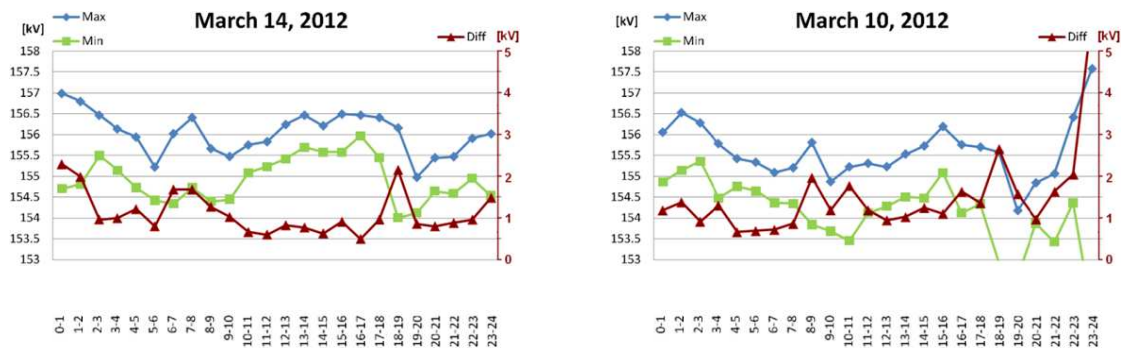
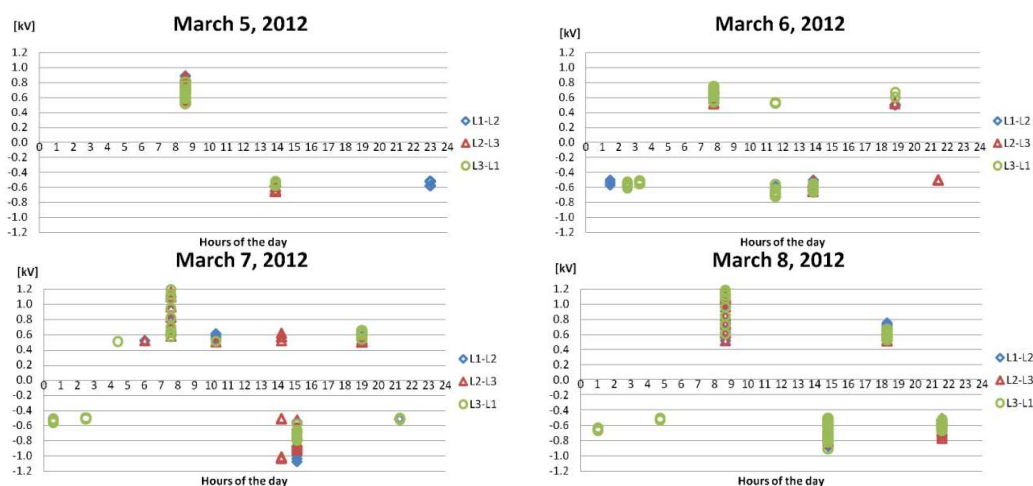


Figure 11. Daily diagrams during the period of 05.03-15.3.2012 for the maximums MIN (blue curves) and for the minimums MAX (green curves) of hourly averaged values of the three voltages (L1, L2, L3) for the 150kV transmission network in Thrace, Greece, as well as their difference DFR (red curves), for each hour of the day. The graphs on March 5 and 14 are representative of magnetically quiet days, with two peaks in the morning and the afternoon. The graphs on March 7 and March 10 are representative of magnetically disturbed days displaying several peaks of comparable values.

In Figure 12 we present high time resolution voltage data of 1 sec from IPTO for the whole period 5-15.3.2015. These data have been processed and presented to examine steep and sudden changes in the high voltage values and we defined as “steep” or “sudden” change in the high voltage, a voltage change greater or less than 500V compared to the current average voltage value in the last 5s (Appendix A). These changes were determined over the course of each day, during the period 5-15.3.2015, and are plotted in the graphs of Figure 12 as overvoltage (positive values) or voltage drop (negative values) points.

From a comparison of the data of Figure 12 with those of Figure 10, we infer that the diagrams of sudden voltage changes (SVC) within 1 sec follows, in general, the standard pattern of the 1-hour averaged voltage data, with almost permanent events in the morning, between 07:00 LT - 09:00 LT and in the evening, between 18:00LT to 20:00LT, but also at post-noon times (14:00LT - 15:00LT), when the citizens have their lunch. We note that the duration of each event, which starts with a sudden voltage increase, is reflected by the number of “anomalous” points (SVC > 500V) than the current average voltage value in the last 5s.



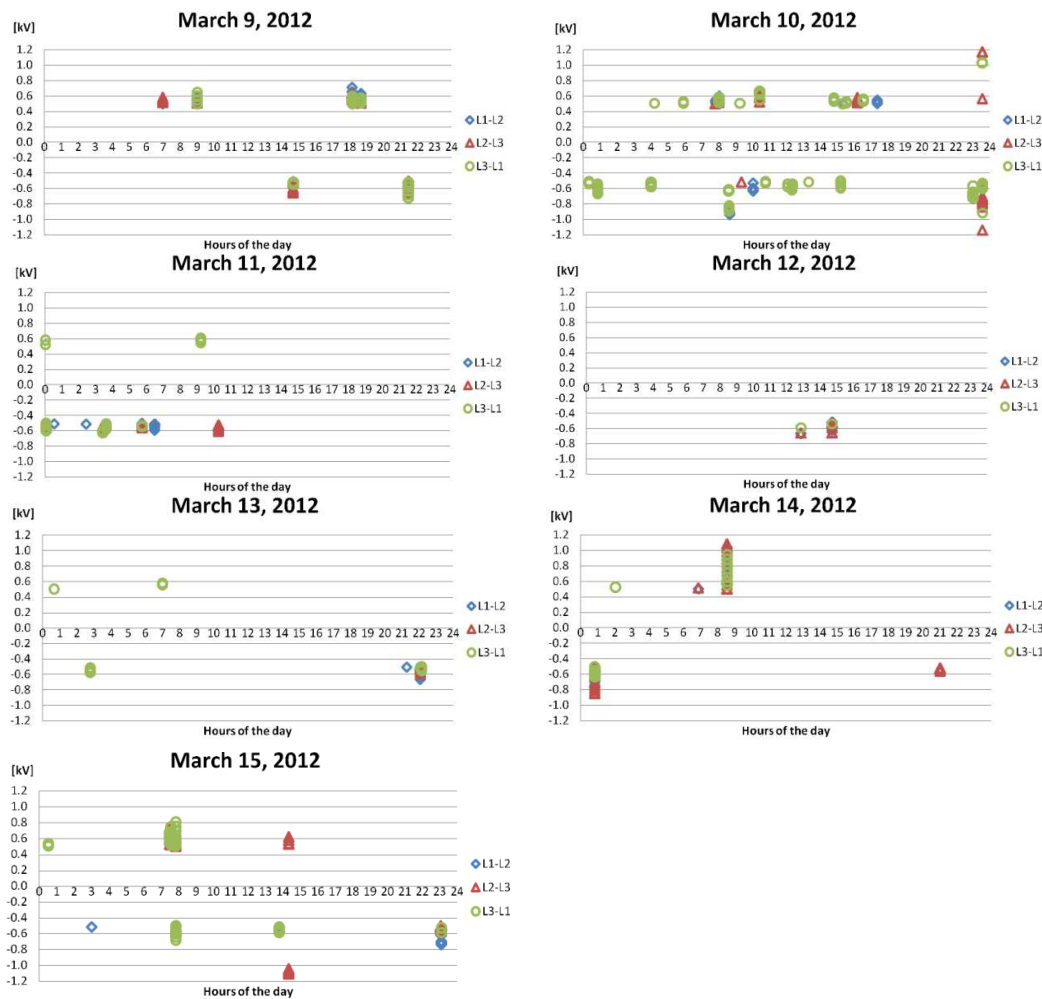


Figure 12. Daily charts (covering the period 5-15.3.2012) for steep and sudden changes for the three phases L1-L2 (blue marks), L2-L3 (red marks) and L3-L1 (green marks) on the transmission network of 150kV in Thrace. Although, the reader can note the moments (morning, noon and evening) that massive human activity is evident, there are points, on some days, which cannot be explained by human activities. It is worth noting that the highest number of anomalous voltage changes were recorded on March 10, during the decay phase (slowly varying magnetic fields) of the major storm in March 2012, observed after the incident of a ICME-related interplanetary shock.

The most characteristic feature revealed from Figures 12 is that SVCs obviously appear in many more times (“anomalous” points) on magnetically disturbed days (7.3.2012 7 and 10.3.2012; Figure 10) than on the quiet days (5.3.2012 and 14.3.2012; Figure 11). For instance an elaboration in Figure 10 suggests that 37 SVCs were recorded on March 10, with maximum daily value of the voltage surges creation / voltage drop 3.61kV / -3.32kV. On the contrary, only 7 SVCs were recorded on March 5, with maximum daily value of the voltage surges creation and the voltage drop 0.89kV / -0.66kV. Detailed information on the daily number of the number of SVCs along with the maximum value of the voltage surges creation and the voltage drop on each day between 5 – 15 March is given in Appendix B. We point out that the results of Figure 10 are in agreement with the results of the hourly averaged data of Figure 11. Furthermore, a comparison between the number of SVC events on days 9.3.2012 and 10.3.2012 suggests that much more sudden disturbances occurred in the electric grid in Thrace on March 10 than on March 9. This is probably an important result, since the magnetic storm on March 10 shows slow geomagnetic field B variation, during the recovery phase of the storm, in contrast to March 9, when the storm is characterized by abrupt B field changes, during the storm main phase (Figures 3 and 13). This result needs further investigation in the future, in order to examine whether such an increased number of SVC events, on electric grids at middle latitudes, is a preferential feature of the recovery decay phase of large storms. We should note that the continuation of the high

occurrence frequency of SVC events until the end of the recovery phase of the storm, that is within the first half of day 11 (Figure 10d), may be an indication of a relation of SVI events on the IPTO electric grid in Thrace with slowly changing geomagnetic fields (Figure 11), which produce quasi-DC electric currents on the ground.

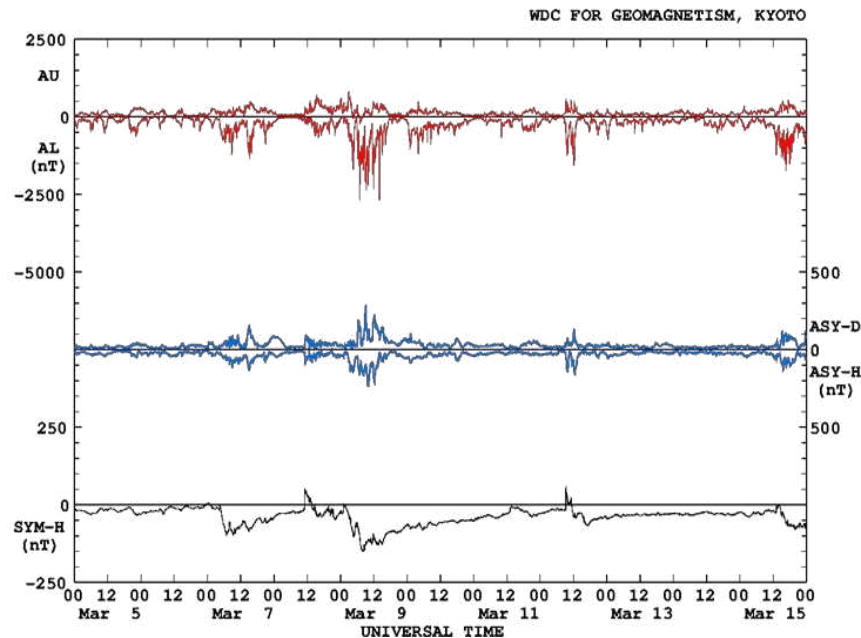
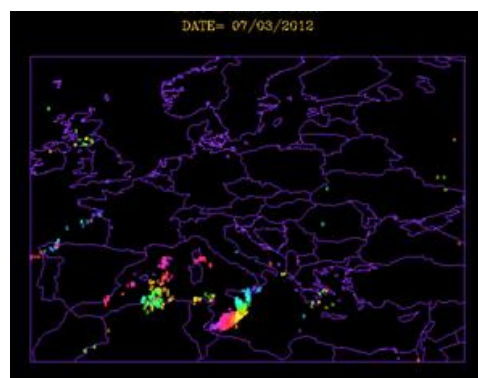


Figure 13. Geomagnetic indexes (AU, AL, ASY-D, ASY-H, SYM-H) during March 5-15, 2012. A series of magnetic storms are seen around 7, 9, 12 and 15 March 2012. The stronger storm lasting from 7 to 11 March was related with the major ICME / SEP event observed by ACE in March 2012 (Figure 3c-3d). The most anomalous voltage events were recorded on March 2010 (Figures 11 and 12) during the decay phase of the major storm in the period examined.

Figure 14 shows lightning records in Greece between 8–10 March 2012. It is evident that no lightning phenomena were recorded in Thrace, northeast Greece, during times with bad weather (intense precipitation, strong wind, great ground electric field fluctuations) and voltage perturbations in the local electric grid, whereas strong lightning activity is evident in the middle Mediterranean on March 10, during strong winds (Figure 7). We infer that the sudden high voltage changes found in the power electric grid in Thrace (Figures 11 and 12), for instance on March 10, cannot be attributed to lightning effects, and they are related with the special space weather conditions at those times. It is worth noting that the lightning activity seen on March 10 was recorded during times of cloudy and anticyclone strong winds (Figure 7).



7.3.2012



8.3.2012

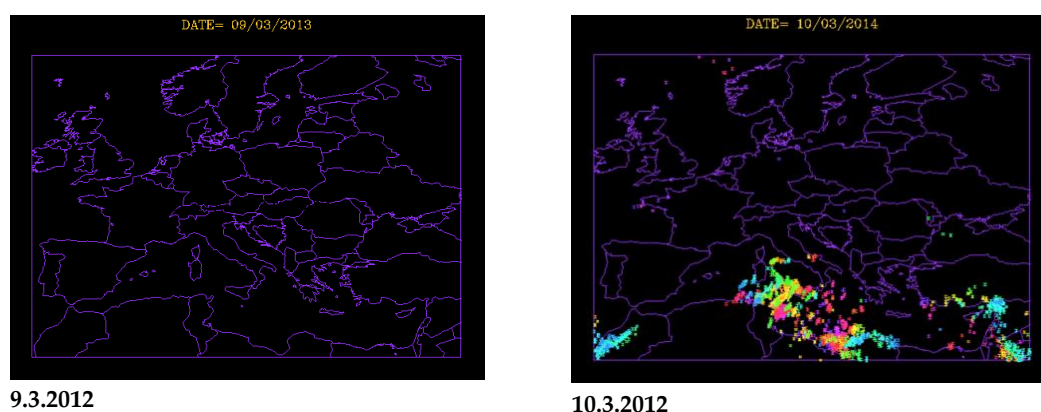


Figure 14. Lightning phenomena in Greece between 7-10 March 2012.

4. Summary of Observations and Discussion

It is well known that the Sun influences Earth's climate and weather. However, there is a need for further research on this topic, in particular, because of the global climate changes of the last two decades. In this perspective, the solar contribution on weather extremes and climate changes should be carefully estimated.

In [4] we presented a case study concerning the possible solar origin of an important extreme event. In particular, in [4] we have demonstrated that the famous March 2012 and the historic March 1910 heatwaves in NE-USA were both occurred during ICME-induced storms. We noted a common extra-terrestrial condition during both the M2012HW and M1910HW. The two heatwaves occurred during the weakest solar cycles (SC) in the last 120 years (SC4 and SC14). Since the M1910HW occurred before the GHG effect and it was evidently a natural, non-anthropogenic, event, [4] inferred that we should accept that the two extreme events (March 2012 and March 1910 heatwaves) had a common origin: solar activity. Furthermore, it is worth noting that the March 2012 heatwave was characterized (i) by the arrival near the Earth of solar cosmic radiation with a proton spectrum extending to unusual high (>0.5 GeV) energies and (ii) a positive North Atlantic Oscillation index. We inferred that the comparison of space and terrestrial data suggests that the hypothesis of a solar influence on the historic March 2012 heatwave cannot be rejected.

Since the March 2012 heatwave was not local in northeast USA, but a global atmospheric anomaly [91], we wanted to further check the possible relation of the unusual solar a7d space weather in March 2012 with meteorological extremes far from the place where the heat wave was experienced. This second case study was selected on the basis of the location of the Demokritos University of Thrace (where most of the co-authors of this paperwork): Thrace, Greece.

To this end we examined a lot of remote sensing instrumentation to investigate likely related physical processes in March 2012 in a variety of space regions: Sun (SDO satellite), Interplanetary Space (ACE satellite), Earth's magnetosphere (Earth based measurements), Top Clouds (TERRA and AQUA satellites), ground atmospheric environment (Earth- based instruments).

Some of the important findings of our research concerning the possible space weather influence on the atmospheric conditions in Thrace, Greece, are the following:

- (1) Unusual bad weather occurred in Thrace, Greece, which started on 6.3. 2012 and lasted until ~15.3. 2012: low temperatures, fast winds and intense precipitation occurred during most of this time period (Figures 3a, 3b, 6–10).
- (2) During the above period (6 – 15.3.2012) of bad weather in Thrace, the ACE satellite recorded high fluxes of solar energetic ions and electrons (Figures 3c and 4), which were related with the presence of a series of ICMEs and magnetic storms (Figures 3d and 13; also [4,14,84]).
- (3) Local measurements in Demokritos University of Thrace, in Xanthi, revealed unusual large amplitude atmospheric electric field E_z fluctuations, after the arrival of two interplanetary shock

waves at ACE, on March 8 and March 11, respectively. Both times of anomalous Ez were followed by storms with intense rainfall and fast winds (Figures 6 and 8).

- (4) The first electric field Ez disturbance on March 8 was the major one, ranging between $\sim 2000\text{V/m}$ - $\sim 1800\text{V/m}$ (Figure 10); the related storm, which lasted in Xanthi from 8 to 11 March 2012, was accompanied by a deep drop in the cloud top temperature as measured by MODIS/TERRA and MODIS/AQUA.
- (5) The winter-like 8 - 10 March 2012 atmospheric events occurred after the detection of the SEP peak flux (8.3.2012; Figure 3c), which accompanying the main ICME that reached the Earth after two intense solar flares on 7 March 2012 (Figure 2 and [4]).
- (6) During the 8 - 10 March 2012 atmospheric event the front of a cyclone appeared in Thrace as a northward jet stream flow, in the direction from the Mediterranean / Aegean Sea to land (Figure 7). MODIS/TERRA measurements suggest that during this period the cloud top temperature drop effect extended to a large range of latitudes, from $\sim 35^\circ\text{N}$ to at least $\sim 70^\circ\text{N}$, with a decreasing effect towards higher latitudes.
- (7) The winter-like 12 - 13 March 2012 jet flow was streaming from the northward direction (higher European latitudes) and it produced highest speeds, but it left no great signal of cloud top temperature drop in MODIS/TERRA and MODIS/AQUA records (Figures 6 and 8). MODIS/TERRA measurements suggest that during this period the cloud top temperature drop effect is more evident at latitudes northward of Xanthi.
- (8) Daily wind fields in south Europe and Mediterranean Sea, including Xanthi, Greece (Figure 6) at mid-tropospheric heights (500 hPa) show that the speed of wind intensifies during two phases (8 - 10.3.2012 and 12 - 13.3.2012) of the continuous course of an eastward moving cyclone appeared on March 6th in east Atlantic / west Mediterranean Sea and left the east Mediterranean / Middle East on March 17th; these two phases of intensified wind speed coincides with periods following the interplanetary shocks of 8 and 11 March.
- (9) During March 2012 precipitation in Alexandroupoli, east Thrace, was recorded during three periods with solar proton flux enhancements at ACE (Figures 3b and 3c).
- (10) Sudden voltage changes (SVCs) within 1 sec ($\text{SVC} > 500\text{V}$ than the current average voltage value in the last 5s) in the high (150 kV) voltage electric power network in Thrace were recorded on magnetically disturbed days (i.e. 7.3.2012 7 and 10.3.2012; Figures 10 and 11).
- (11) Many more sudden voltage disturbances occurred in the electric grid in Thrace on March 10 than on March 9 indicating a preference for the recovery phase of the storm (Figures 12 and 13). In the following we will refer to the above conclusions 1 - 12 as Points #1 -12.

4.1. March 2012 space weather and atmospheric extremes in Thrace, Greece,

The present second case study dealing with the possible relationship of the solar / space activity with extreme atmospheric events in March 2012 allows to make important conclusions on the possible agent of winter-like weather in Thrace, Greece.

Point #1 compared with the results of [4] allows the hypothesis that the unusual March 2012 heat wave in northeast USA and the bad weather in northeast Greece, which started on the same day, 6 March, 2012, may have the same agent. In addition, Points #2 - 6 and #8-9 suggest that the periods of March 2012 with bad weather in Thrace occurred after SEP events observed earlier in the interplanetary space by the ACE satellite (as in the case of March 2012 heat wave in northeast USA).

In particular, Points #3 - 6 and Point #8 suggest that the highly geoeffective ICME-related SEP event [4], with a flux peak on 8 March 2012 was most probably the agent of the extreme weather event occurred on 8-10 March 2012 in Thrace, Greece, and in the east Mediterranean as well. The space origin of the 8-10 March 2012 extreme meteorological event is greatly supported by the fact that, throughout a long-lasting eastward moving cyclone (6 - 17 March) in Mediterranean Sea, the wind speed became highest only during periods (8-10 and 12-13 March 2012) following the incident of two interplanetary waves / solar cosmic ray / into the Earth's magnetosphere. The detailed meteorological measurements made in Xanthi suggest that the large electric field fluctuations, rainfall

and winds on March 8 started after >1.5 days from the occurrence of the solar flare of March 7, in agreement to the early results of Schuurmans [33].

It is worth noting that the 8-10 March 2012 extreme event in Thrace was related with a deep drop in CTT, which extended to a long range of middle and latitudes ($\sim 35^{\circ}$ - 70° N at Xanthi longitude). The CTT deviation recorded by MODIS/TERRA on 8-10 March 2012 decreased with increasing latitude and it was evidently a result of northward streaming air flows from the Aegean Sea / Mediterranean (Point#6). The cyclone being in progress at those times in the whole Mediterranean, at longitudes between -10° W to $\sim 28^{\circ}$ E (Figure 6) and the CTT deviation between $\sim 35^{\circ}$ - 70° N (Point#6) reveal that the bad weather in northeast Greece examined in the present paper was a part of a large scale weather anomaly. This conclusion is in agreement with the well-known fact that the a global weather anomaly was in progress on the planet after 7 March 2012 [4, 91], when solar cosmic rays started arriving at the Earth's environment due to the two large solar flares occurred at the beginning of the same day (Point #5).

In [4] we discussed the March 2012 magnetic superstorm in reference of a set of 28 large magnetic storms occurred between August 1997 and March 2015. The set of these storms was selected by using as a selection the minimum value of the geomagnetic index Dst during the March 2012 magnetic superstorm (Dst = -150 nT); the set of the storms was collected under the criterion $\text{Dst} \leq -150\text{nT}$, that was a set of storms larger than the March 2012 magnetic superstorm, in a period of about 18 years. The March 2012 storm-related SEP event was characterized by the fact that the ACE satellite recorded the highest energetic (1.88–4.70 MeV) proton intensity j ($j > 10^4 \text{ p (cm}^2 \cdot \text{sec. sr. MeV)}^{-1}$) and peak-to-background value $j_p/j_b > 10^6$; Figure 3c) among all 28 SEP events related with the largest (Dst < -150 nT) magnetic storms examined in [4].

This special feature of the March 2012 ICME may suggest that the solar cosmic rays and not the magnetic storm was the agent of the extreme weather in Greece, as we claimed in the case of the March 2012 heat wave in USA [4]. It is worth noting that other satellites, like SOHO and PAMELA, measuring protons at high energies, recorded protons with spectrum extending much above 500 MeV [86, 96].

Visbeck et al found that during a positive NAO (North Atlantic Oscillation), conditions are warmer and wetter than average in northern Europe, the eastern United States, and parts of Scandinavia, whereas conditions are colder and drier than average over the northwestern Atlantic and Mediterranean regions [97, 98]. In [4] we argued that the positive NAO mediated the effect of the SEP event on March 2012 heatwave in USA. Since the March 2012 bad weather in northeast Greece was an aspect of a large scale weather activity including a region from west Mediterranean / west Atlantic to Middle East (Point #8; Figure 6) it is possible that positive NAO might be hypothesized to be responsible for the east Mediterranean / Aegean Sea fast air flow recorded after the major SEP event on 8-10 March 2012, although other physical mechanisms cannot be excluded. For instance, the unusual the unusual strong energetic electron precipitation in the cusp (Figure 4) may also influenced the AEF fluctuation and bad weather on 8-10 and 11-12 March, 2012 in Xanthi (Thrace)[75]. Definitely, the possible relationship of NAO with atmospheric conditions in Greece and east Mediterranean is an important topic for further research.

Finally, we should point out that our study on March 2012 weather in Thrace revealed variations in electric conditions. In particular we confirmed the presence of two types of electric disturbances at those times: (i) large amplitude atmospheric electric field variations at the beginning of rainfall on March 8 and March 11 (Point 4), and (ii) voltage variations in the electric power network in Thrace on March 10, 2012, during the decay phase of the magnetic storm [Point #11].

4.2. Sudden Voltage Changes on the electric power grid in Thrace, Greece, in March 2012

Voltage anomalies were recorded in the electric grid in Thrace, Greece, during the magnetic storm on March 7, 2012 and during the recovery phase of the major storm on 10 and 11 March. The abrupt voltage variations in the electric grid in Thrace at a time period following the arrival of a greatly geoeffective ICME on March 7 and its associated SEP event on March 7-9, should be

understood as a result of the slowly varying geomagnetic field and the induced electric currents at those times (Figs. 3 and 11-12).

Problems in transformers and electric grids as a result of some intense solar flares and ICMEs is a phenomenon that has attracted the interest of space research and various states over the last decades and remote sensing space weather research has been used to predict possible dangerous geoeffective effects and protect human societies and technical systems. To this end several states have established special organizations or supported institutional research on GIC and their effects on power networks. For instance, the United States have supported this kind of research with the Federal Energy Regulatory Commission, the National Space Weather Strategy and the National Space Weather Action Plan [National Science and Technology Council, 2015]. In Australia the Power Transmission Network Service Providers cooperated with the Australian Energy Market Operator and the Australian Bureau of Meteorology to install some equipment to record GIC effects on some transformers in the Australian electric network [99]. In the United Kingdom, the GICs constitute the space weather element in the National Risk Registry [100].

Many other states or individual researchers have conducted systematic research on GIC effects on electric networks at high, middle and low, as in New Zealand [101], South Africa [102-104], China [105, 106], Brazil [107], Malaysia [108], Uruguay [109]. Similar studies have also been conducted in Mexico [110], Spain [111], Portugal [112] and Ethiopia [113].

Furthermore, the ACE and SOHO satellites located at the Lagrangian point L1 between Sun and Earth as well as the observations of the Sun by space based telescopes (i.e. AIA instrument on the SDO satellite used in the present study) have been extensively used to detect space weather and predict unusual magnetospheric and atmospheric phenomena. In addition, NOAA provides almost real-time data from ACE, which provides information ~1 hour before the time that an intense ICME can cause catastrophic GIC effects on electric networks. Solar, space and ground measurements are combined to predict dangerous space weather conditions and protect electric networks. [114] has pointed out that medium GICs can provoke premature aging to the equipment of High Voltage transformer.

We should point out that there is good evidence that the voltage anomalies recorded in northeast Greece in March 2012 were related with the magnetic field variation during the storms of 7th and 9th-11th of March. Firstly, at those times, no lightning activity was recorded in Thrace, Greece, Secondly, the intense solar particle streaming, which was most probably the agent of the meteorological extreme in the period after the ICME arrival at Earth on 7-9.3.2012, was not the agent of the voltage disturbances in the electric grid. This conclusion is supported by the fact that the highest occurrence frequency of SVCs were recorded on March 10-11, 2012, much later than the high energy solar particle flux maximum on March 8, 2012 (Figure 3c). Since the SVCs in Thrace were recorded during the two major storms in March 2012 (7 and 9 to 11), the SVCs can be attributed to the magnetic storm activity. Furthermore, we claim that we can separate the different agents of the March 2012 extreme meteorological events and of the voltage anomalies in the electric power grid in Thrace, Greece, in the course of ICME interaction with the Earth's physical / technological environment.

Two mechanisms can cause changes in the high voltage of the 150kV transmission network: (1) the generation of voltage drops caused by arcing between high voltage lines and the Earth, as result of short-circuits, and voltage crossing to the Earth, due to the varying magnetic field during storms between the high voltage lines and the Earth, (2) surges creation (anomalous voltage increases), due to penetration of DC currents created by a CME-induced storm and consequently diffused from the ground into the transformers of the high voltage electric power grid [9].

It is possible that the large number of voltage drops that appeared on 7 and 10-11 March 2012 in the electric grid of Thrace, Greece, operating by the IPTO factory in Komotini, is due to high voltage arcs from cables to Earth or other conductive elements. These voltages arcs from cables to Earth may result either from an increase of magnetic field between cables and Earth or from an increase in the Earth's electric field. Any voltage arcing from cables to Earth, depending on the current passed to the Earth, is capable of causing the recorded voltage drops. The surges might be the result of an increase

in storm induced quasi-DC electric field at Earth, through which the transmitted current is likely to have affected the high-voltage transformers, with the mechanism explained in Appendix D.

It is worth noting that many more sudden disturbances in the electric grid in Thrace occurred during the recovery phase of the March 2012 storm (Figs. 10 and 11), which may suggest a preference of this phenomenon for slowly varying (quasi-DC) fields. A similar pattern can also be seen in the cases of the Geomagnetically Induced Currents estimated during the August and November 2018 magnetic storms recently studied by Hughes et al [115; their Figures 3 and 14].

5. Conclusions

The influence of solar activity on Earth's climate is a well-known phenomenon [1, 2, 11, 19, 116, 117]. Most studies have been devoted so far to investigate the solar cycle effects on the ionosphere, the stratosphere and the troposphere, while only few case studies have been published examining the short-time effects of solar activity on the atmospheric dynamics and the weather extremes.

Echer et al. found a very significant correlation ($r \approx 0.6-0.8$) in the ~22 year-solar cycle between the sunspot number and the latitudinal averaged surface temperatures [118]. However, there is good evidence that the solar activity produces different surface temperature responses at different latitudes and longitudes [33, 37, 119]. Therefore, different weather (i.e. temperature) responses to strong solar activity is expected.

In this perspective, we extended our previous study [4] on the possible causal relation between the unusual space weather variations and the famous March 2012 heatwave in America, by comparing the solar / space weather variations with the bad weather in Thrace, Greece, for the same time period (March 2012). To this end, we compared data from a lot of remote sensing experiments and we investigated physical processes in March 2012 on the Sun, the Interplanetary Space, the Earth's magnetosphere, the top of the clouds and the near ground atmosphere.

The comparison of this variety of data, all the way from the Sun to the Earth's ground, allowed us to conclude that there is good evidence on the influence of the unusual geoeffective solar activity and space weather conditions between 6 – 14 March 2012 [14, 118] on the extreme weather events in Thrace, Greece. Here, it is worth noting the impressive information given by an ESA report: «Already in ancient Greece, around 400 B.C., Meton observed sunspots (Hoyt and Schatten, 1997). After twenty years of solar studies he came to the conclusion that solar activity, i.e high number of sunspots, is associated with wet weather in Greece. Today the observations of Meton could have been associated with the changes of the North Atlantic Oscillation (NAO) (Hurrell et al., 2003)» [120]. Indeed, the March 2012 bad weather in Greece occurred during times of increased positive NAO index [4; Figure 5].

The analysis of data demonstrated that the winter-like weather in Thrace on 7 – 14 March was an aspect of large scale weather anomalies taking place all over the north Europe, the Mediterranean Sea, the southeast Europe, the Aegean Sea and the southeast European countries.

A comparison of the features of 28 large (<150nT) ICME-related magnetic storms during a period of ~18 years (1997-2015) implied the conclusion that the solar cosmic rays were most probably the main agent of the solar impact on the early March 2012 winter-like weather events in Thrace, Greece, as it was suggested in the study on March 2012 heatwave in USA [4], which started on the same day (March 6). This conclusion is in agreement with the results of Pudovkin and Raspopov [38] and Pudovkin and Babushkina [39], that the main extraterrestrial agent of weather variations in the lower atmosphere is the solar and galactic cosmic ray radiation.

The relationship between space and physical processes in two such distant regions on the planet, as USA [4] and Greece (present study), strongly supports the hypothesis of the significant role of solar activity in triggering the low troposphere weather in March 2012 in Thrace, Greece. Furthermore, the fact that the space weather-related March 1910 and March 2012 heatwaves in USA were an aspect of global atmospheric anomalies suggests that the special solar activity was most probably the agent of the two historic events [121].

Our conclusion that the March 2012 heatwave in USA [4] and the winter-like weather in Greece at the same time period were the results of a common agent may have important implications in fully

understanding some of the weather changes and, therefore, it needs further examination, in particular in our times, when the frequency of extreme weather events has been increased and the need for estimating anthropogenic versus physical contribution in climate change appears to be of the highest importance. Furthermore, the results of the present paper suggests that detailed case studies based on multi-instrument high time (i.e. #min /hour / day) resolution data are important in extracting hidden information from extreme weather events.

Finally, we reported, for the first time, sudden (within 1 second) voltage changes in an electric power network at middle latitudes, namely in the power network of Thrace / Greece, located at ~41°N. During the March 2012 magnetic storm important voltage changes in the electric grid were recorded during the decay phase of the magnetic storm. Although the amplitude of the voltage fluctuations was rather small (maximum voltage surge at 3.61kV and voltage drop at -3.32kV on March 10), this effect may be important under different geomagnetic / geophysical conditions and in higher latitude electric power grids. Definitely, the novel finding of geomagnetically induced voltage changes in electric grids opens a new window into space weather applications research.

Author Contributions: Conceptualization, G.A. and A.K.; methodology, G.A. and A.K.; software, A.K., S-A.I.M., D.O., N. Ch.; validation, G.A. and M.D.; formal analysis, G.A. and S-A.I.M.; investigation, G.A.,A.K., D.E., and D.O.; data curation, G.A., A.K., S-A.I.M., D.O., S.K., N.Ch; writing—original draft preparation, G.A., A.K., P.M.; writing—review and editing, G.A.,D.E., P.M., A.K., M.D.; visualization, A.K., S-A.I.M., D.O., N.Ch; supervision, G.A., M.D.; funding acquisition, G.A. All authors have read and agreed to the published version of the manuscript.

Funding: This research received no external funding.

Acknowledgments: The first author (G.A.) thanks L. Lanzerotti for providing the ACE/EPAM energetic particle data as well as K. Kourtidis for providing meteorological data (Figure 8) from the Laboratory of Air Pollution and Pollution Control Engineering of Atmospheric Pollutants, Dept. of Environmental Engineering, Democritus University of Thrace, Xanthi, Greece, and TERRA/MODIS data processing as well as V. Kotroni for helping us to extract useful information from the National Observatory of Athens /ZEUS LITHTNING DATA. G.A.also thanks K. Kourtidis for helpful discussions and his comments on a preliminary version of the present manuscript. The authors acknowledge the use of data from: theWeatherOnline Services (1), the World Data Center for Geomagnetism, Kyoto (2), AIA instrument onboard the SDO satellite from heliviewer.org /(3), the MODIS (Moderate Resolution Imaging Spectroradiometer) instrument on the satellites TERRA and AQUA, produced with the Giovanni online data system, developed and maintained by the NASA GES DISC (4) NOAA, NCEP (National Centers for Environmental Prediction) and (5) and NOAA satellites (NOAA 18 /19). 1. <http://www.weatheronline.co.uk/weather/maps/forecastmaps?LANG=en&CONT=ukuk&R=150;> 2. <https://wdc.kugi.kyoto-u.ac.jp/dstdir>; 3. <https://heliviewer.org/>; 4. <https://giovanni.gsfc.nasa.gov/giovanni/>; 5.<https://www.weather.gov/ncep/>

Conflicts of Interest: The authors declare no conflict of interest.

Appendix A

The detection of sudden voltage variations (voltage increase and voltage decrease) was achieved according to the algorithm:

$$\Delta V_n = V_n - (V_n + V_{n-1} + V_{n-2} + V_{n-3} + V_{n-4})/5 , \tag{A1}$$

where, $\Delta V_n > 0.5kV$ (for voltage increase) or $\Delta V_n < -0.5kV$ (for voltage decrease).

Appendix B

Table A1. The number of SVC events Nsvc between 5-15.3.2012. The number of sudden voltage drops and surges creation in the electric power in Thrace, Greece, was highest on 10.3.2012, during the decay phase of the major magnetic storm in March 2012 (Figs 3 and 11). In addition, the highest values of the sudden voltage drop and the surges creation were recorded on the same day.

Date	# Sudden Voltage Change Events	Maximum Surges Creation (kV)	Maximum Voltage Drop (kV)
------	--------------------------------	------------------------------	---------------------------

	Nsvc		
5/3/2012	7	0.89	-0.66
6/3/2012	22	0.75	-0.73
7/3/2012	22	1.47	-1.08
8/3/2012	25	1.19	-0.91
9/3/2012	24	0.71	-0.72
10/3/2012	37	3.61	-3.32
11/3/2012	16	0.61	-0.63
12/3/2012	6	0.00	-0.67
13/3/2012	9	0.58	-0.67
14/3/2012	12	1.08	-0.85
15/3/2012	23	0.80	-1.11

Appendix C

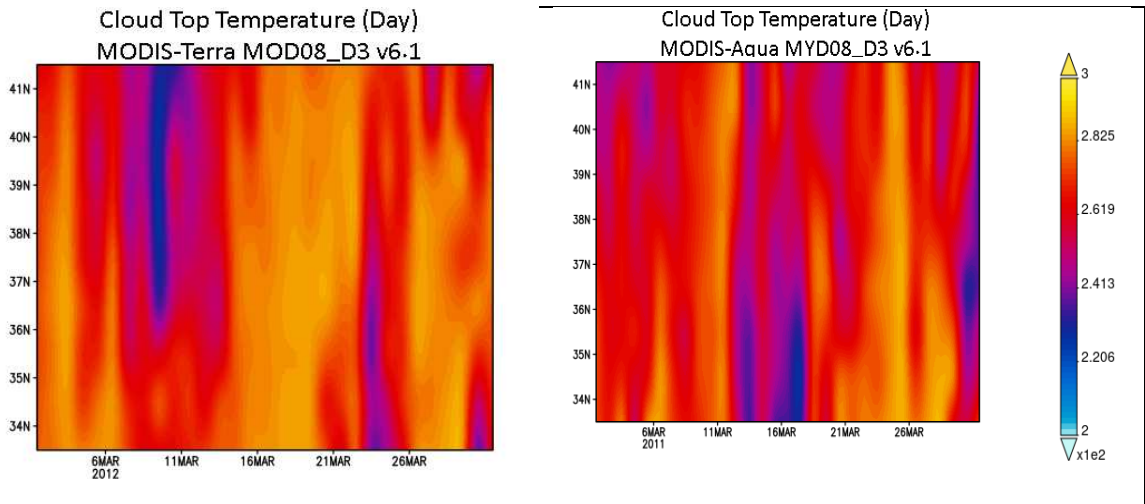


Figure A1. Data in the same format as in Figure5, but for a year before (March 2011). MODIS CTT maps for the same region as in Figure 5 show no similarities to the 2012 MODIS CTT.

Appendix D

Figure A2 shows that the vertices of the positive portions of the AC waveform are five times higher due to the effect of the DC current.

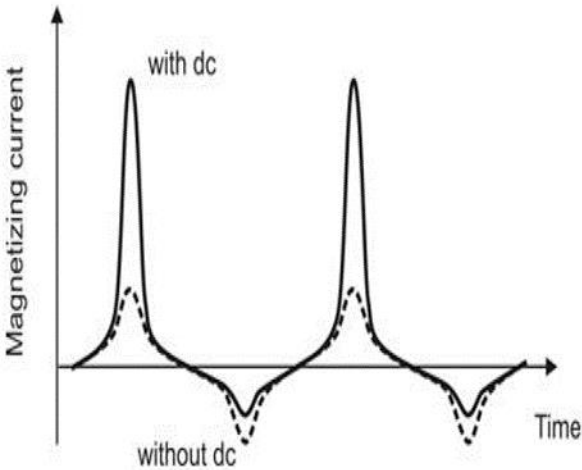


Figure A2. Effect of induced DC current on the transformer current [30].

References

- Shindell, D.T.; Schmidt, G.A.; Mann, M.E.; Rind, D.; Waple, A. Solar Forcing of Regional Climate Change during the Maunder Minimum. *Science* 2001, 294, 2149–2152. doi:10.1126/science.1064363.
- Easterbrook, D. The Solar Magnetic Cause of Climate Changes and Origin of the Ice Ages; 3rd ed. Independently Publisher: Washington, DC, USA, 2019.
- Avakyan, S.V.; Voronin, N.A.; Nikol'sky, G.A. Response of Atmospheric Pressure and Air Temperature to the Solar Events in October 2003. *Geomagn. Aeron.* 2015, 55, 1180–1185. doi:10.1134/S0016793215080034
- Anagnostopoulos, G.C.; Menesidou, S.-A. I.; Efthymiadis, D.A. The March 2012 HeatWave in Northeast America as a Possible Effect of Strong Solar Activity and Unusual Space Plasma Interactions. *MDPI Atmosphere*. 2022, 13, 6, 926. <https://doi.org/10.3390/atmos13060926>.
- Coumou, D.; Rahmstorf, S. A Decade of Weather Extremes. *Nat. Clim. Chang.* 2012, 2, 491–496. DOI:10.1038/NCLIMATE1452
- Robine, J.-M.; Cheung, S.L.K.; Roy, S.L.; Oyen, H.V.; Griffiths, C.; Michel, J.-P.; Herrmann, F.R. Death Toll Exceeded 70,000 in Europe during the Summer of 2003. *Comptes Rendus Biol.* 2008, 331, 171–178. DOI: 10.1016/j.crv.2007.12.001
- CarbonBrief, Attributing Extreme Weather to Climate Change. Available online: <https://www.carbonbrief.org/mapped-howclimate-change-affects-extreme-weather-around-the-world> (accessed on 1 March 2022).
- Dole, R.; Hoerling, M.; Perlwitz, J.; Eischeid, J.; Pegion, P.; Zhang, T.; Quan, X.-W.; Xu, T.; Murray, D. Was There a Basis for Anticipating the 2010 Russian HeatWave? *Geophys. Res. Lett.* 2011, 38, L06702. <https://doi.org/10.1029/2010GL046582>
- Kumar, A.S.; Chen, M.; Hoerling, M.; Eischeid, J. Do Extreme Climate Events Require Extreme Forcings. *Geophys. Res. Lett.* 2013, 40, 3440–3445. <https://doi.org/10.1002/grl.50657>
- Love, J.; Hayakawa, H.; Cliver, E. On the Intensity of the Magnetic Superstorm of September 1909. *Space Weather*. 2019, 17, 37–45. <https://doi.org/10.1029/2018SW002079>
- Connolly, R.; Soon, W.; Connolly, M.; Baliunas, S.; Berglund, J.; Butler, C.J.; Cionco, R.G.; Elias, A.G.; Fedorov, V.M.; Harde, H.; et al. How Much Has the Sun Influenced Northern Hemisphere Temperature Trends? An Ongoing Debate. *Res. Astron. Astrophys.* 2021, 21, 131. DOI: 10.1088/1674-4527/21/6/131
- Hundhausen, A.J. Coronal Expansion and Solar Wind; Springer-Verlag Berlin Heidelberg New York, 1972.
- Richardson, I.G. Solar wind stream interaction regions throughout the heliosphere, *Liv. Rev. Sol. Phys.* 2018, 1, 15., <https://doi.org/10.1007/s41116-017-0011-z>.
- Patsourakos, S.; Georgoulis, M.K.; Vourlidis, A.; Nindos, A.; Sarris, T.; Anagnostopoulos, G.C.; Anastasiadis, A.; Chintzoglou, G.; Daglis, I.A.; Gontikakis, C.; et al. The major geoeffective Solar eruptions of 2012 March 7: Comprehensive Sun-to-Earth analysis. *Astrophys. J.* 2016, 817, 14. DOI: 10.3847/0004-637X/817/1/14
- Barnes, A. Solar-Terrestrial Physics: Principles and Theoretical Foundations; edited by R.L. Carovillano, and J.M. Forbes (D. Reidel Publishing Company, Dordrecht, 1983), 155-199.
- Kumar, A.; Badruddin, B. Study of the evolution of the geomagnetic disturbances during the passage of high-speed streams from coronal holes in solar cycle 2009-2016. *Astrophys. and Space Sci.* 2021, 366(2). doi:10.1007/s10509-021-03927-5.
- Abdu, M. A.; de Souza, J. R.; Sobral, J. H. A.; Batista, I. S. Magnetic Storms Associated Disturbance Dynamo Effects in the Low and Equatorial Latitude Ionosphere. *Geophys. Res. Ser.* 2006, 167, Recurrent Magnetic Streams, Washington, DC, AGU 2006, 283–304. doi:10.1029/167gm22
- Prikryl, P.; Ghoddousi-Fard, R.; Thomas, E.G.; Ruohoniemi, J.M.; Shepherd, S.G.; Jayachandran, P.T.; Danskin, D.W.; Spanswick, E.; Zhang, Y.; Jiao, Y.; Morton, Y.T. GPS phase scintillation at high latitudes during geomagnetic storms of 7–17 March 2012 – Part 1: The North American sector. *Ann. Geophys.* 2015, 33, 637–656. doi:10.5194/angeo-33-637-2015
- Gray, L.J.; Beer, J.; Geller, M.; Haigh, J.D.; Lockwood, M.; Matthes, K.; Cubasch, U.; Fleitmann, D.; Harrison, G.; Hood, L.; et al. Solar Influence on Climate. *Rev. Geophys.* 2010, 48, RG4001. doi:10.1029/2009RG000282.
- Herman, J.R.; Goldberg, R.A. Sun Weather and Climate; Dover Pub Inc., New York, 1978.
- Anagnostopoulos, G.C.; Spyroglou, I.; Rigas, A.; Preka-Papadema, P.; Mavromichalaki, H.; Kiosses, I. The sun as a significant agent provoking earthquakes. *European Phys. J. Special Topics*. 2021, 230, 287–333 <https://doi.org/10.1140/epjst/e2020-000266-2>.
- Anagnostopoulos, G.C.; Papandreou, A. Space conditions during a month of a sequence of six M > 6.8 earthquakes ending with the tsunami of 26 December 2004. *Nat. Hazards Earth Syst. Sci.* 2012, 12, 1551–1559. <https://doi.org/10.5194/nhess-12-1551-2012>
- Duma, G.; Ruzhin, Y. Diurnal changes of earthquake activity and geomagnetic Sq-variations. *Nat. Hazards Earth Syst. Sci.* 2003, 3, 171–177. <https://doi.org/10.5194/nhess-3-171-2003>
- Zenchenko, T.A.; Breus, T.K. The Possible Effect of Space Weather Factors on Various Physiological Systems of the Human Organism. *Atmosphere*. 2021, 12, 346. <https://doi.org/10.3390/atmos12030346>.

25. Vencloviene, J.; Babarskiene, R.; Slapikas, R. The association between solar particle events, geomagnetic storms, and hospital admissions for myocardial infarction. *Nat. Hazards*. 2013, 65, 1-12.
26. Noula, M.; Preka-Papadema, P.; Moussas, X.; Vassiliou, Ch.; Tsaliki, S.-M.; Kontogeorgou, E.; Katsavrias, Ch.; Theodoropoulou, A. Recorded Cases at the Emergency Department of the General Hospital of Lamia Town during the Year 2005 in Association with Helio-geomagnetic Activity. *Hellenic J. of Nursing Sci.* 2010, 3, 53-62.
27. Palmer, S.J.; Rycroft, M.J.; Cermack, M. Solar and geomagnetic activity, extremely low frequency magnetic and electric fields and human health at the Earth's surface. *Surveys in Geophysics*. 2006, 27, 557-595. <https://doi.org/10.1007/s10712-006-9010-7>
28. Lanzerotti, L.J. Space Weather: Historical and Contemporary Perspectives. *Space Sci Rev.* 2017, 212, 1253–1270. <https://doi.org/10.1007/s11214-017-0408-y>.
29. Marhavilas, P.K. The Space Environment and its Impact on Human Activity. CSEG RECORDER. *Canadian Soc. of Explor. Geophys.* 2004, 41-50.
30. Kirkham, H.; Makarov, Y.V.; Dagle, J.E.; DeSteese, J.G.; Elizondo, M.A.; Diao, R. Geomagnetic Storms and Long-Term Impacts on Power Systems. Pacific Northwest National Laboratory, Richland, Washington 99352, 2011. <https://doi.org/10.2172/1059627>
31. Labitzke, K.; Kunze, M.; Brönnimann, S. Sunspots, the QBO and the Stratosphere in the North Polar Region 20 Years Later. *Meteorol. Z.* 2006, 15, 355–363. DOI: 10.1127/0941-2948/2006/0136.
32. Raspopov, O.; Veretenenko, S. Solar Activity and Cosmic Rays: Influence on Cloudiness and Processes in the Lower Atmosphere (in Memory and on the 75th Anniversary of M.I. Pudovkin). *Geomagnet. and Aeronomy*. 2009, 49, 137–145. DOI:10.1134/S0016793209020017
33. Schuurmans, C.J.E. Tropospheric Effects of Variable Solar Activity. *Sol. Phys.* 1981, 74, 417–419. DOI:10.1007/BF00154527
34. Pudovkin, M.I. Influence of Solar Activity on the Lower Atmosphere State. *Int. J. Geomagn. Aeron.* 2004, 5, GI2007. DOI:10.1029/2003GI000060
35. Siingh, D.; Singh, R.P.; Singh, A.K.; Kulkarni, M.N.; Gautam, A.S.; Singh, A.K. Solar Activity, Lightning and Climate. *Surv. Geophys.* 2011, 32, 659-703. DOI:10.1007/s10712-011-9127-1
36. Le Mouél, J.-L.; Lopes, F.; Courtillot, V. A. Solar Signature in Many Climate Indices. *J. Geophys. Res. Atmos.* 2019, 124, 2600–2619. DOI:10.1029/2018JD028939
37. Kossobokov, V.; Mouél, J.L.; Courtillot, V. On the Diversity of Long-Term Temperature Responses to Varying Levels of Solar Activity at Ten European Observatories. *Atmosph. and Climate Sci.* 2019, 9, 498–526. DOI: 10.4236/acs.2019.93033
38. Pudovkin, M.I.; Raspopov, O.M. A mechanism of solar activity influence on the state of the lower atmosphere and meteoroparameters. *Geomagn. Aeron.* 1992, 32, 1–9.
39. Pudovkin, M.I.; Babushkina, S.V. Influence of Solar Flares and Disturbances of the Interplanetary Medium on the Atmospheric Circulation. *J. Atmos. Terr. Phys.* 1992, 54, 841–846. [https://doi.org/10.1016/0021-9169\(92\)90050-U](https://doi.org/10.1016/0021-9169(92)90050-U)
40. Smirnov, S.E.; Mikhailova, G.A.; Kapustina, O.V. Variations in Electric and Meteorological Parameters in the Near-Earth's Atmosphere at Kamchatka during the Solar Events in October 2003. *Geomagn. Aeron.* 2014, 54, 240–247. DOI:10.1134/S0016793214020182
41. Mironova, I.A.; Usoskin, I.G. Possible Effect of Strong Solar Energetic Particle Events on Polar Stratospheric Aerosol: A Summary of Observational Results. *Environ. Res. Lett.* 2014, 9, 015002. DOI:10.1088/1748-9326/9/1/015002
42. Tinsley, B.A.; Deen, G.W. Apparent Tropospheric Response to MeV-GeV Particle Flux Variations: A Connection via Electrofreezing of Supercooled Water in High-Level Clouds? *J. Geophys. Res.* 1991, 96, 22283–22296. <https://doi.org/10.1029/91JD02473>
43. Marsh, N.; Svensmark, H. Cosmic Rays, Clouds, and Climate. *Space Sci. Rev.* 2000, 94, 215–230. DOI:10.1023/A:1026723423896
44. Roldugin, V.; Tinsley, B.A. Atmospheric Transparency Changes Associated with SolarWind-Induced Atmospheric Electricity Variations. *J. Atmos. Sol.-Terr. Phys.* 2004, 66, 1143–1149. <https://doi.org/10.1016/j.jastp.2004.05.006>
45. Bazilevskaya, G.A.; Usoskin, I.G.; Flückiger, E.O.; Harrison, R.G.; Desorgher, L.; Büttikofer, R.; Krainev, M.B.; Makhmutov, V.S.; Stozhkov, Y.I.; Svirzhetskaya, A.K.; Svirzhetsky, N.S.; Kovaltsov, G.A. Cosmic Ray Induced Ion Production in the Atmosphere. *Space Sci. Rev.* 2008, 137, 149–173. <https://doi.org/10.1007/s11214-008-9339-y>
46. Boteler, D.H. *Space Weather Effects on Power Systems*. Space Weather Geophys. Monogr. Ser. 2001, 125, edited by P. Song, H. J. Singer, and G. L. Siscoe, 347–352, AGU, Washington, D.C.
47. Kappenman, J. Geomagnetic Storms and Their Impacts on the U.S. Power Grid. Metatech Corporation, Goleta, Calif 93117, January 2010. Available online: http://web.ornl.gov/sci/ees/etsd/pes/pubs/ferc_Meta-R-319.pdf (accessed on 26 July 2015)

48. Kappenman, J.G. The Evolving Vulnerability of Electric Power Grids, *Space Weather*. 2004, 2, 1. <https://doi.org/10.1029/2003SW000028>.
49. Kappenman, J.G.; Albertson, V.D. Bracing for the geomagnetic storms. *IEEE Spectrum*, 1990, 27, 27-33.
50. Kappenman, J.G. Advanced geomagnetic storm forecasting for the electric power industry. *Space Weather, Geophys. Monogr. Ser.* 125, edited by P. Song, H. J. Singer, and G. L. Siscoe, 353–358, AGU, Washington, D.C., 2001. doi:10.1029/GM125p0353.
51. Thomson, A. Space weather and power grids. *Earthwise* 2010, 26, British Geological Survey, NERC, https://geomag.bgs.ac.uk/documents/Earthwise_26_powergrids.pdf.
52. Liu, J.; Wang, C. B.; Liu, L.; Sun, W.-H. The response of local power grid at low-latitude to geomagnetic storm: An application of the Hilbert Huang transform. *Space Weather*. 2016, 14, 300–312. doi:10.1002/2015SW001327.
53. Nicoll, K.A. Space weather influences on atmospheric electricity. *Weather* 2014, 69, pp. 238–241. ISSN 1477-8696 doi: <https://doi.org/10.1002/wea.2323>,
54. American Meteorological Society, Glossary of Meteorology, https://glossary.ametsoc.org/wiki/Atmospheric_electric_field.
55. Bennett, A.J.; Harrison, R.G. Variability in surface atmospheric electric field measurements. *J. Phys.: Conf. Ser.* 2008, 142 012046. DOI 10.1088/1742-6596/142/1/012046
56. Li, L.; Chen, T.; Ti, S.; Wang, S.-H.; Song, J.-J.; Cai, C.-L.; Liu, Y.-H.; Li, W.; Luo, J. Fair-Weather Near-Surface Atmospheric Electric Field Measurements at the Zhongshan Chinese Station in Antarctica. *Appl. Sci.* 2022, 12, 9248. <https://doi.org/10.3390/app12189248>
57. Troshichev, O.A.; Frank-Kamenetsky, A.; Burns, G.; Fuellekrug, M.; Rodger, A.; Morozov, V. The relationship between variations of the atmospheric electric field in the southern polar region and thunderstorm activity. *Adv. Space Res.* 2004, 34, 1801–1805. DOI:10.1016/j.asr.2003.07.063
58. Whipple, F.J.W. Modern views on atmospheric electricity. *Q.J. R. Meteorol. Soc.* 2007, 64, 199–222. DOI:10.1002/qj.49706427502
59. Liu, C.; Williams, E.R.; Zipser, E.J.; Burns, G. Diurnal Variations of Global Thunderstorms and Electrified Shower Clouds and Their Contribution to the Global Electrical Circuit. *J. Atmos. Sci.* 2010, 67, 309–323.
60. Tinsley, B.A.; Burns, G.B.; Zhou, L. The role of the global electric circuit in solar and internal forcing of clouds and climate. *Adv. Space Res.* 2007, 40, 1126–1139. DOI:10.1016/j.asr.2007.01.071
61. Telang, A.V.R. The influence of rain on the atmospheric-electric field. *J. Geophys. Res.* 1930, 35, 125–131.
62. Yan, M.; Shen, Q.; Zhou, C. Atmospheric electric field at ground in partial region in China. *Plateau Meteorol.* 1988, 2, 156–165.
63. Tacza, J.; Raulin, J.P.; Mendonça, R.; Makhmutov, V.; Marun, A.; Fernandez, G. Solar Effects on the Atmospheric Electric Field During 2010–2015 at Low Latitudes. *J. Geophys. Res. Atmos.* 2018, 123, 11–970.
64. Zhang, H.; Zhang, Y.; Yang, S. Characteristics of atmospheric electric field in Taiyuan and its relationship with atmospheric pollutants. *Environ. Sci. Technol.* 2013, 36, 66–69.
65. Li, J.; Chen, X.; Cheng, Y.; Li, R.; Dong, F. Preliminary Study on the Relationship between Atmospheric Electric Field and Air Pollutants in Beijing. *Plateau Weather*. 2021, 40, 209–218.
66. Huang, Y.; Wu, A.; Zhang, S. Influence of environmental features on the atmospheric electric field and correction. *Electron. Meas. Technol.* 2018, 41, 35–38.
67. Gurmani, S.F.; Ahmad, N.; Tacza, J.; Iqbal, T. First seasonal and annual variations of atmospheric electric field at a subtropical station in Islamabad, Pakistan. *J. Atmos. Sol.-Terr. Phys.* 2018, 179, 441–449.
68. Zhou, Y.; Chen, C.P.; Liu, L.P.; Chu, R.Z.; Feng, J.M.; Zhang, T.; Song, X.M.; Kajikawa, M.; Fujii, H.Y.; Aoi, T.; et al. Atmospheric electric field in hail weather system in Naqu area of Qinghai-Tibet Plateau. *Plateau Weather*. 2000, 3, 339–347
69. Zhang, Y.; Meng, Q. Atmospheric Electricity Characteristics in the Eastern Qinghai-Tibet Plateau. *Plateau Weather*. 1998, 17, 135–141.
70. Yan, M.; Xiao, Q. Analysis of the characteristics of the atmospheric electric field in the western Pacific Ocean from September to November in 1988. *Plateau Weather*. 1990, 9, 395–404.
71. Choudhury, A.; Guha, A.; De, B.K.; Roy, R. A statistical study on precursory effects of earthquakes observed through the atmospheric vertical electric field in northeast India. *Ann. Geophys.* 2013, 56, R0331.
72. Smirnov, S. Association of the negative anomalies of the quasistatic electric field in atmosphere with Kamchatka seismicity. *Nat. Hazards Earth Syst. Sci.* 2008, 8, 745–749.
73. Chen, T.; Zhang, X.X.; Zhang, X.M.; Jin, X.B.; Wu, H.; Ti, S.; Li, R.K.; Li, L.; Wang, S.H. Imminent estimation of earthquake hazard by regional network monitoring the near surface vertical atmospheric electrostatic field. *Chin. J. Geophys.* 2021, 64, 1145–1154.
74. Pulnits, S.; Boyarchuk, K. Ionospheric Precursors of Earthquakes. Springer, ISBN3-540-20839-9, 2004.
75. Kleimenova, N.G.; Gromova, L.I.; Gromov, S.V.; Malysheva, L.M. Large Magnetic Storm on September 7–8, 2017: High-Latitude Geomagnetic Variations and Geomagnetic Pc5 Pulsations. *Geomagn. Aeron.* 2018, 58, 597–606. DOI:10.1134/S0016793218050080

76. Michnowski, S.; Odzimek, A.; Kleimenova, N.G.; Kozyreva, O.V.; Kubicki, M.; Klos, Z.; Israelsson, S.; Nikiforova, N.N. Review of Relationships Between Solar Wind and Ground-Level Atmospheric Electricity: Case Studies from Hornsund, Spitsbergen, and Swider, *Poland. Surv. Geophys.* 2021, 42, 757–801. DOI:10.1007/s10712-021-09639-3
77. Pesnell, W.D.; Thompson, B.J.; Chamberlin, P.C. The Solar Dynamics Observatory (SDO). *Sol. Phys.* 2012, 275, 3–15. DOI: 10.1007/s11207-011-9841-3
78. Stone, E.C.; Burlaga, L.F.; Cummings, A.C.; Feldman, W.C.; Frain, W.E.; Geiss, J.; Gloeckler, G.; Gold, R.E.; Hovestadt, D.; Krimigis, S.M.; Mason, G. M.; McComas, D.; Mewaldt, R. A.; Simpson, J. A.; von Rosenvinge, T. T.; Wiedenbeck, M. The Advanced Composition Explorer. *AIP Conf. Proc.* 1990, 203, 48–57.
79. EOS, NASA' Earth Observing System, Terra, <https://eosso.nasa.gov/missions/terra>. (29.11. 2023).
80. NASA, Aqua Project Science, <https://aqua.nasa.gov/content/about-aqua> (29.11. 2023).
81. NASA, MODIS (Moderate Resolution Imaging Spectroradiometer). <https://modis.gsfc.nasa.gov/> (30.11.2023).
82. NS ENERGY, Komotini Combined-Cycle Power Plant, <https://www.nsenergybusiness.com/projects/komotini-combined-cycle-power-plant/#> (30.11.2023).
83. World Data Center for Geomagnetism, Geomagnetic Equatorial Dst index Home Page, Kyoto, <https://wdc.kugi.kyoto-u.ac.jp/dst/dir/> (30.11.2023).
84. Tsurutani, B.T.; Echer, E.; Shibata, K.; Verkhoglyadova, O.P.; Mannucci, A.J.; Gonzalez, W.D.; Kozyra, J.; Pätzold, M. The Interplanetary Causes of Geomagnetic Activity during the 7–17 March 2012 Interval: A Cawses II overview. *J. Space Weather Space Clim.* 2014, 4, 8. <https://doi.org/10.1051/swsc/2013056>.
85. Maragkakis, M.G.; Anagnostopoulos, G.C.; Vassiliadis, E.S. Upstream Ion Events with Hard Energy Spectra: Lessons for Their Origin from a Comparative Statistical Study (ACE/Geotail). *Planet. Space Sci.* 2013, 85, 1–12.
86. Kühl, P.; Dresing, N.; Heber, B.; Klassen, A. Solar Energetic Particle Events with Protons Above 500 MeV Between 1995 and 2015 Measured with SOHO/EPHIN. *Sol. Phys.* 2017, 292, 10.
87. Papaioannou, A.; Souvatzoglou, G.; Paschalis, P.; Gerontidou, M.; Mavromichalaki, H. The First Ground-Level Enhancement of Solar Cycle 24 on 17 May 2012 and Its Real-Time Detection. *Sol. Phys.* 2014, 289, 423–436.
88. Gurnett, D.A.; Kurth, W.S.; Burlaga, L.F.; Ness, N.F. In Situ Observations of Interstellar Plasma with Voyager 1. *Science.* 2013, 341, 1489–1492.
89. Zeitlin, C.; Hassler, D.M.; Cucinotta, F.A.; Ehresmann, B.; Wimmer-Schweingruber, R.F.; Brinza, D.E.; Kang, S.; Weigle, G.; Böttcher, S.; Böhm, E.; Burmeister, S.; Guo, J.; Köhler, J.; Martin, C.; Posner, A.; Rafkin, S.; Reitz, G. Measurements of Energetic Particle Radiation in Transit to Mars on the Mars Science Laboratory. *Science.* 2013, 340, 1080–1084. DOI: 10.1126/science.1235989
90. Tsurutani, B. T.; McPherron, R. L.; Gonzalez, W. D.; Lu, G.; Gopalswamy, N.; Guarnieri, F. L. Magnetic Storms Caused by Corotating Solar Wind Streams, in Recurrent Magnetic Storms: Corotating Solar Wind. *Geophysical Monographs.* AGU 2006, 167. doi:10.1029/167GM03
91. Dole, R.; Hoerling, M.; Kumar, A.; Eischeid, J.; Perlwitz, J.; Quan, X.-W.; Kiladis, G.; Webb, R.; Murray, D.; Chen, M.; et al. The making of an extreme event: Putting the Pieces Together. *Bull. Am. Meteorol. Soc.* 2014, 95, ES57–ES60.
92. Hanna, J.; Schultz, D; Irving, A. Cloud-Top Temperatures for Precipitating Winter Clouds. *J. Applied Meteor. Climat.* 2008, 47(1), 351–359.
93. Kastelis, N.; Kourtidis, K. Characteristics of the atmospheric electric field and correlation with CO2 at a rural site in southern Balkans. *Earth Planets and Space.* 2016, 68,(1):3 DOI:10.1186/s40623-016-0379-3
94. Nicoll, K.; Harrison, R. G.; Bor, J.; Barta, V.; Brugge, R.; Chillingarian, A.; Chum, J.; Georgoulas, A.; Guha, A.; Kourtidis, K.; Kubicki, M.; Mareev, E.; Matthews, J.; Mkrtchyan, H.; Odzimek, A.; Raulin, J. -P.; Robert, D.; Silva, H. G.; Tacza, J.; Yair, Y.; Yaniv, R. A global atmospheric electricity monitoring network for climate and geophysical research. *J. Atmosph. Solar-Terr. Physics* 2019, 184, 18–29.
95. Mikhailova, G.A.; Kapustina, O.V.; Smirnov, S.E. Effects of solar and geomagnetic activities in variations of power spectra of electrical and meteorological parameters in the near-Earth atmosphere in Kamchatka during October 2003 solar events. *Geomagn. Aeron.* 2014, 54,5, 645–654. doi:10.1134/S0016793214050119.
96. Bazilevskaya, G.A.; Mayorov, A.G.; Mikhailov, V.V. Comparison of Solar Energetic Particle Events Observed by PAMELA Experiment and by Other Instruments in 2006–2012. In *Proceedings of the Internat. Cosmic Ray Conf.*, Rio de Janeiro, Brazil 2013, 33, 1392.
97. Woollings, T.; Lockwood, M.; Masato, G.; Bell, C.; Gray, L. Enhanced signature of solar variability in Eurasian winter climate. *Geophys. Res. Lett.* 2010, 37, L20805, doi:10.1029/2010GL044601.
98. Visbeck, M.H.; Hurrell, J.W.; Polvani, L.; Cullens, H.M. The North Atlantic Oscillation: Past, present, and future. *Proceedings of the National Academy of Sciences* 2001, 98, 23,12876–12877 DOI:10.1073/pnas.231391598

99. Marshall, R.A.; Kelly, A.; Van Der Walt, T.; Honecker, A.; Ong, C.; Mikkelsen, D.; Spierings, A.; Ivanovich, G.; Yoshikawa, A. Modeling geomagnetic induced currents in Australian power networks. *Space Weather*. 2017, 15, 7. <https://doi.org/10.1002/2017SW001613>
100. Cabinet Office; National Risk Register of Civil Emergencies. 2015 [Available at: https://assets.publishing.service.gov.uk/government/uploads/system/uploads/attachment_data/file/419549/20150331_2015-NRR-WA_Final.pdf]
101. Divett, T.; Richardson, G. S.; Beggan, C. D.; Rodger, C. J.; Boteler, D. H.; Ingham, M.; MacManus, D.H.; Thomson, A.W.P.; Dalzell, M. Transformer-level modeling of geomagnetically induced currents in New Zealand's South Island. *Space Weather*. 2018, 16, 718–735. <https://doi.org/10.1029/2018SW001814>.
102. Koen, J.; Gaunt, T. Geomagnetically induced currents in the Southern African electricity transmission network. *Proc. IEEE Bologna Power Tech. Conf.* 2003, 7.
103. Gaunt, C.T.; Coetzee, G. Transformer failures in regions incorrectly considered to have low GIC-risk. *IEEE Lausanne Power Tech. Proceedings*, 2007, Lausanne, Switzerland, 1–5 July 2007, 807–812.
104. Torta, J. M.; Marsal, S.; Quintana, M. Assessing the hazard from geomagnetically induced currents to the entire high-voltage power network in Spain. *Earth Planets and Space* 2014, 66, 1–17. <https://doi.org/10.1186/1880-5981-66-87>.
105. Liu, C. M.; Liu, L. G.; Pirjola, R.; Wang, Z. Z. Calculation of geomagnetically induced currents in mid- to low-latitude power grids based on the plane wave method: A preliminary case study. *Space Weather* 2009, 7, S04005. <https://doi.org/10.1029/2008SW000439>.
106. Zheng, K.; Liu, L. G.; Ge, H. Y.; Li, W. X. Comparative study of the GIC amplitudes and characteristics in different power grids in China. *CIGRE* 2012, C3–206.
107. Trivedi, N. B.; et al. Geomagnetically induced currents in an electric power transmission system at low latitudes in Brazil: A case study, *Space Weather* 2007, 5, S04004. doi:10.1029/2006SW000282.
108. Zawawi, A.A.; Ab Aziz, N.F.; AbKadir, M.Z.A.; Hashim, H.; Mohammed, Z. Evaluation of Geomagnetic Induced Current on 275 kV Power Transformer for a Reliable and Sustainable Power System Operation in Malaysia. *Sustainability* 2020, 12, 9225. <https://doi.org/10.3390/su12219225>.
109. Caraballo, R.; SánchezBettucci, L.; Tancredi, G. Geomagnetically induced currents in the Uruguayan high-voltage power grid. *Geophys. J. International* 2013, 195, 2, 844–853. <https://doi.org/10.1093/gji/ggt293>
110. Caraballo, R.; González-Esparza, J. A.; Sergeeva, M.; Pacheco, C. R. First GIC estimates for the Mexican power grid. *Space Weather* 2020, 18, 2, <https://doi.org/10.1029/2019SW002260>.
111. Torta, J. M.; Marsal, S.; Quintana, M. Assessing the hazard from geomagnetically induced currents to the entire high-voltage power network in Spain. *Earth Planets and Space*. 2014, 66(1), 1–17. <https://doi.org/10.1186/1880-5981-66-87>.
112. Ribeiro, J. A.; Pinheiro, F. J. G.; Pais, M. A.; Santos, R.; Cardoso, J.; Baltazar-Soares, P.; Monteiro Santos, F. A. Toward more accurate GIC estimations in the Portuguese power network. *Space Weather*. 2023, 21, e2022SW003397. <https://doi.org/10.1029/2022SW003397>.
113. Abraha, G.; Yemane, T.; Kassa, T. Geomagnetic storms and their impacts on Ethiopian power grid. *Advances in Astronomy and Space Physics* 2020, 10, 55–64 doi: 10.17721/2227-1481.10.55-64
114. Molinski, T.S. Why utilities respect geomagnetically induced currents. *J. Atmos. Sol.-Terr. Phys.* 2002, 64, 1765.
115. Hughes, J.; Mcgranaghan, R.; Kellerman, A. C.; Bortnik, J.; Arrit, R. F.; Venkataramani, K.; Perry, C.H.; McCormick, J.; Ngwira, C.M.; Cohen, M. Revealing novel connections between space weather and the power grid: Net-work analysis of ground-based magnetometer and Geomagnetically Induced Currents (GIC) measurements. *Space Weather*. 2022, 20, e2021SW002727. <https://doi.org/10.1029/2021SW002727>
116. Gleisner, H.; Thjll, P. Patterns of tropospheric response to solar variability. *Geophys. Res. Lett.* 2003, 30, 13, 44-1 – 44-4. doi:10.1029/2003GL017129.
117. Gray, G.; Scaife, A.; Mitchell, D.; Osprey, S.; Ineson, I.; Hardiman, S.; Butchart, N.; Knight, J.; Sutton, R.; Kodera, K., A lagged response to the 11 year solar cycle in observed winter Atlantic/European weather patterns, *J. Geophys. Res.* 2013, 118, 13, 405–13, 420, doi:10.1002/2013JD020062.
118. Echer, S.; Echer, E.; Rigozo, N.; Brum, C.; Nordeman, D.; Gonzalez, W. The relationship between global, hemispheric and latitudinal averaged air surface temperature (GISS time series) and solar activity, *J. of Atmosph. and Solar-Terr. Phys.* 2012, 74, 87–93.
119. Maliniemi, V., T. Asikainen, K. Mursula, and A. Seppälä, QBO-dependent relation between electron precipitation and wintertime surface temperature. *J. Geophys. Res. Atmos.*, 2013, 118, 6302–6310, doi:10.1002/jgrd.50518.
120. Bober, F.; Lundstedt, H. and Winoft, P. Influence of Solar Activity Cycles on Earth's Climate. *ESA ITT AO/1-4618/NL/AR*, 2005.
121. Ouzounov, D.; Anagnostopoulos, G.C.; Menesidou, S.-A. I.; Karkanis, A.; Efthymiadis, D.A.; Kampatagis, A.; Marhavilas, P.; Danikas, M. Side of a global weather extreme in March 2012, the heat wave in North-East America and the extreme cold weather in South-East Europe as possible effects of intense solar activity. *AGU Meeting*, 2022, NH14C-05. <https://agu.confex.com/agu/fm22/meetingapp.cgi/Paper/1139675>.

Disclaimer/Publisher's Note: The statements, opinions and data contained in all publications are solely those of the individual author(s) and contributor(s) and not of MDPI and/or the editor(s). MDPI and/or the editor(s) disclaim responsibility for any injury to people or property resulting from any ideas, methods, instructions or products referred to in the content.